

TRANSIENT VIBRATION

OF

THIN RECTANGULAR CANTILEVER PLATES

Thesis submitted for the Degree of

Master of Science of the

University of Edinburgh

by

Edward M. Forsyth B.Sc.

August 1959



## Acknowledgements

The author wishes to express his thanks to Professor R.N. Arnold for providing the opportunity and facilities for the work, and to Dr. G. B. Warburton for his suggestion of the problem and his guidance throughout the investigation.

## CONTENTS

Chapter 1	<u>Introduction</u> .....	pp. <b>1-8</b>
Chapter 2	<u>Calculation of Natural Frequencies</u> <u>and Modes of Vibration</u> .....	pp. <b>9-31</b>
2.1.	Uniform Beams	<b>9.</b>
2.1.1.	Solution of the Equation of Motion	<b>9.</b>
2.1.2.	Rayleigh (Energy) Method	<b>10.</b>
2.2.	Rectangular Cantilever Plates	<b>12.</b>
2.2.1.	The Plate Equation of Motion	<b>12.</b>
2.2.2.	Nodal Patterns	<b>14.</b>
2.2.3.	Rayleigh Method	<b>14.</b>
2.2.4.	Rayleigh-Ritz Method	<b>19.</b>
2.2.5.	The variational Method	<b>23.</b>
2.2.6.	The Finite-difference Approach	<b>24.</b>
2.2.7.	Comparison of the various methods for calculating natural frequencies	<b>27.</b>
Chapter 3	<u>Impact and Transient Vibrations</u> ..pp	<b>32-46</b>
3.1.	Historical Introduction	<b>32.</b>
3.2.	Vibration of a Plate	<b>36.</b>
3.2.1.	Arbitrary force distribution	<b>36.</b>
3.2.2.	Force concentrated at a point.	<b>38.</b>

3.2.3.	Impact of a sphere on the plate: The Integral Equation.	41.
3.2.4.	An approximate solution of the impact problem	43.
Chapter 4.	<u>Experiments and Calculations</u> .....pp	47-54
4.1.	The Plate and Clamping Device	47.
4.2.	Determination of Natural Frequencies	47.
4.3.	Transient Displacements	49.
4.4.	Transient Strains	53.
Chapter 5.	<u>Comments and Conclusions</u> .....pp	55-68
Appendix 1.	<u>Application of Calculus of Variations to minimise equation (17)</u> .....pp	69-72
Appendix 2.	<u>References</u> .....pp	73-76
Appendix 3.	<u>Notation</u> .....pp	77-79
Table 1.	<u>Coefficients for Cantilever Plate for use in Warburton's method.</u> pp	17.
Table 2.	<u>Experimental and Calculated Frequencies for rectangular cantilever Plate</u> .....pp	82.
Figure 1.	Coordinate axes and Plate Dimensions	13.
Figure 2.	Nodal Pattern: $m=3; n=2$ .	15.
Figure 3.	Grid Pattern for Finite-differences	25.
Figure 4.	Development of the Integral Equation	40.
Figure 5.	Plate Dimensions and Clamping arrangement.	80.
Figure 6.	Determination of natural frequencies and Recording of Transient Displacements.	81.
Figure 7.	Displacement at $(16", 7\frac{1}{2}"$ )	83.
Figure 8.	Displacement at $(16", 0"$ )	84.

Figure 9.	Recording of Transient Strains	85.
Figure 10.	Strain at (0.64", 1.875")	86.
Figure 11.	Strain at (0.64", 3.75")	87.
Figure 12.	Displacement at (16", 7 $\frac{1}{2}$ ") using experimental frequencies	88.
Figure 13.	Displacement at (16", 0") using experimental frequencies	89.
Figure 14.	Strain at (0.64", 1.875") using experimental frequencies	90.
Figure 15.	Strain at (0.64", 3.75") using experimental frequencies	91.

TRANSIENT VIBRATIONS OF THIN, RECTANGULAR,  
CANTILEVER PLATES.

CHAPTER 1                      INTRODUCTION

When an elastic structure is subjected to a static load the deformation produced is independent of time and is a state of equilibrium between the applied load and the elastic properties of the system.

Where dynamic loads are involved the state of equilibrium is no longer independent of time but includes the effects of the inertial forces due to the motion of the system. Only in certain cases does the deformation of the structure retain a particular shape while varying in magnitude. In general both the deflection at a given point and the shape of the deformation throughout the system are time-dependent.

The eventual failure of a structural component may be due to metal fatigue, rather than the actual values of stresses associated with the dynamic loads since a vibration may continue to exist for some time after removal of the load.

The sources of dynamic loads depend on the types of structures considered and the uses to which they are put, but the following cases illustrate a few of the possibilities and some of the structures affected.

1. Shock waves due to explosions, earthquakes, etc.
  - (a) In an internal-combustion engine the piston/

2.

piston and cylinder are subjected to a rapid series of explosive forces and the piston also has a high inertia loading due to its motion as a rigid body.

(b) The pressure wave associated with a nuclear explosion is accompanied by a strong thermal shock wave.

(c) In countries where earthquakes are relatively common occurrences the building codes contain allowances for their effects.

## 2. Moving loads

Bridges are vibrated by the movement of traffic across them. Railway bridges especially are subject to very heavy loading due to the weights of the vehicles and also the "hammer blow" effects connected with the peculiar balancing conditions employed on steam locomotives.

3. Water waves produce impulsive loads on the bows of a ship and vessels used for ice-breaking work under conditions of dynamic loading.

4. The forces acting on an aeroplane in flight can change rapidly due to maneuvering or encountering turbulent air, and at the moment of landing severe impact loads are transmitted to the fuselage and wings through the landing gear.

The/

The importance of the stresses produced in this latter case is well illustrated by the photograph at the beginning of the book "Dynamics of Airplanes" by H. N. Abramson. This shows a large aeroplane on the ground with both wings broken at the roots. The legend accompanying the photograph is the formula for stresses produced by a sudden load!

The present problem was suggest by the lack of its consideration in the literature, either theoretically or experimentally.

Greenspon (1955) studied the deflections and stresses induced by transient loading in plates with simply supported or clamped edges, and obtained an approximate formula for the maximum deflection and stress. No experimental results were available but static deflections and stresses were compared with published results given by Timoshenko (1940) for some combinations of clamped and supported edges. Part of the analysis requires the calculation of natural frequencies of transverse vibration of the plate and Greenspon states that the method he employs can be used for plates with free, supported or clamped edges. The expression he uses is based on the differential equation of motion for the plate (see equation (35), Chapter 3) and requires the approximate deflection shape to satisfy the boundary conditions at the edges of the plate. The approximating/



4.

approximating functions used by Greenspon do satisfy the conditions for supported or clamped edges but not those for free edges. Frequencies calculated by this method for cases with free edges can be either higher or lower than the true frequencies. This is especially true for a cantilever plate which has three free edges, the approximate frequency differing from the experimental value by a very wide margin.

Chapter 2 of this dissertation is devoted to a discussion of methods suitable for calculating the natural frequencies of plates.

Eringen (1953) considered the impact of a sphere on a plate or beam from the integral equation standpoint. (See Chapter 3, Section 3.2.3) The paper is mainly concerned with the calculation by various approximate methods of the variation with time of the force between the sphere and the plate. Plates with free edges are not treated.

To obtain data for comparison with calculated results it was necessary to carry out an experiment in which some form of transient loading could be applied to a cantilever plate. In the actual choice of an experimental set-up several methods of initiating a transient vibration were considered which had been used by various workers in studying vibrations of beams.

1. E. Z. Stowell, E.B. Schwartz and J.C. Houbolt  
(1945).

This group of authors investigated the results obtained by the instantaneous arrest of/  
of/

of the root of a moving cantilever beam.

"A circular steel tube was mounted symmetrically on the end of a pendulum to form a pair of cantilever beams. The pendulum was permitted to start its swing from a predetermined position and was suddenly brought to rest at the bottom of its swing against an electromagnet used to prevent rebound."

Assuming that the motion of the cantilevers immediately before impact could be considered as uniform translation perpendicular to their lengths, the authors developed a theory for the bending and shear stresses produced in the beams by the impact.

If the beams were replaced by plates it might not be permissible to neglect the effects of air resistance and the finite breadth of the plate would cause a variation of velocity across it.

## 2. G. A. Nothmann (1948)

The "free" end of a cantilever beam was forced to follow a prescribed displacement law and expressions were obtained for the shear force and displacement at any point in the beam. The investigation was mainly concerned with the force necessary to produce the prescribed motion. i.e. The magnitude and direction of the shear force at the "free" end/

6.

end of the beam. No experimental results are quoted.

It would be difficult to apply this method to a cantilever plate since twisting of the plate could occur about an axis perpendicular to the clamped edge.

3. R. P. N. Jones (1954)

The method used by Jones is mathematically similar to that of Stowell, et al, in that a sudden disturbance is applied to the system, in this case sudden removal of a static load.

A simply supported beam was held in an initial position of static deflection by a magnet and coil arrangement. The coil was attached to the beam at its midpoint and release of the beam was effected by cutting off the current passing through the coil.

4. R. H. MacNeal (1951) used an analogue approach to study the natural frequencies and mode shapes of a cantilever plate. The relevant differential equation was expressed in finite difference form and the solution was obtained from the currents and voltages in the analogue network.

Transient vibration of plates could be solved in this way but MacNeal suggests that a reasonably complicated problem would require about 250 essentially perfect transformers.

Previous/

Previous papers by McCann and MacNeal (1950) and by Criner, McCann and Warren (1945) studied the transient vibration problems of beams and finite degree-of-freedom systems respectively.

An advantage of electrical analogue experiments is that various odd-shaped pulses can be applied to disturb the system and non-uniformity of the system itself can be considered.

5. The method that was finally adopted was that of impact of a steel sphere falling from a height on to the plate. Little apparatus was required, the parameters of the process could be varied quickly (e.g. position of impact, etc.) and, as will be shown in Chapter 3, for the corresponding problem of impact on beams an approximate solution exists which can be employed in the present problem.

In the analysis of vibration of a plate two of the most important factors are the natural frequencies and modes of vibration of the plate. Approximate calculation of these quantities is described in Chapter 2.

Chapter 3 contains the mathematical analysis of the transient vibration of a cantilever plate, produced by an arbitrary load distribution, and also considers the particular case of a concentrated force (as applied to the impact problem).

Experimental/

Experimental and calculated results are given in Chapter 4. The final chapter summarises these results and discusses possible extensions which could be made in the analysis.

For free, undamped, harmonic vibration of a uniform beam the transverse displacement  $w$  at any point  $x$  along the beam satisfies the partial differential equation

$$\frac{\partial^4 w}{\partial x^4} + \frac{1}{c^2} \frac{\partial^2 w}{\partial t^2} = 0 \quad (1)$$

If  $w = W(x) \sin \omega t$  this reduces to the ordinary differential equation

$$\frac{d^4 W}{dx^4} - \frac{\omega^2}{c^2} W = 0 \quad (2)$$

where  $\omega$  is the  $n^{\text{th}}$  natural frequency of the beam and  $c = \sqrt{\frac{E I}{\rho A}}$  is a constant for a given beam.

Putting  $K = \frac{\omega}{c}$ , the solution of equation (2) is of the form

$$W = A \cosh Kx + B \sinh Kx + C \cos Kx + D \sin Kx \quad (3)$$

where  $A, B, C$  and  $D$  are constants to be evaluated from the conditions at the ends of the beam. Such boundary conditions are

$$\left. \begin{aligned} W = \frac{dW}{dx} = 0 \quad \text{at } x = \text{clamped end} \\ \frac{d^2 W}{dx^2} = \frac{d^3 W}{dx^3} = 0 \quad \text{at } x = \text{free end} \end{aligned} \right\} \quad (4)$$

The first pair of equations (4) are known as geometrical or artificial conditions and the second pair are the boundary or natural conditions.

Substitution of the correct boundary conditions

## 2. Calculation of Natural Frequencies and Normal Modes of Vibration

### 2.1. Uniform Beams

#### 2.1.1. Solution of the Equation of Motion

For free, undamped, harmonic vibration of a uniform beam the transverse displacement  $w$  at any point  $x$  along the beam satisfies the partial differential equation

$$\frac{\partial^4 w}{\partial x^4} + \frac{1}{c^2} \cdot \frac{\partial^2 w}{\partial t^2} = 0 \quad (1)$$

If  $w = W_r(x) \sin \omega_r t$  this becomes the ordinary differential equation

$$\frac{d^4 W_r}{dx^4} - \frac{\omega_r^2}{c^2} \cdot W_r = 0 \quad (2)$$

where  $\omega_r$  is the  $r^{\text{th}}$  natural frequency of the beam and  $c = \sqrt{\frac{EIg}{AP}}$  is a constant for a given beam.

Putting  $K_r = \sqrt{\frac{\omega_r}{c}}$ , the solution of equation (2) is of the form

$$W_r = A \cosh K_r x + B \cos K_r x + C \sinh K_r x + D \sin K_r x \quad (3)$$

where A, B, C and D are constants to be evaluated from the constraints at the ends of the beam. Such boundary conditions are

$$\left. \begin{aligned} W_r = \frac{dW_r}{dx} = 0 & \text{ at a clamped end} \\ \frac{d^2 W_r}{dx^2} = \frac{d^3 W_r}{dx^3} = 0 & \text{ at a free end} \end{aligned} \right\} \quad (4)$$

The first pair of conditions (4) are known as geometrical or artificial conditions and the second pair are the dynamical or natural conditions.

Substitution of the correct boundary conditions

in equation (3) leads to values for  $B/A$ ,  $C/A$ ,  $D/A$  and to a "frequency equation", the roots of which are related to the natural frequencies of the beam.

Examples are:

1. Beam clamped at  $x = 0$  and free at  $x = l$

$$W_T = (\cosh K_T x - \cos K_T x) - \sigma_T (\sinh K_T x - \sin K_T x) \left. \begin{array}{l} \text{where} \\ \sigma_T = \frac{\sinh K_T l - \sin K_T l}{\cosh K_T l + \cos K_T l} \\ \text{and} \\ \cosh K_T l \cdot \cos K_T l + 1 = 0 \end{array} \right\} \quad (5)$$

2. Beam free at both ends.

$$W_T = (\cosh K_T x + \cos K_T x) - \sigma_T (\sinh K_T x + \sin K_T x) \left. \begin{array}{l} \text{where} \\ \sigma_T = \frac{\cosh K_T l - \cos K_T l}{\sinh K_T l - \sin K_T l} \\ \text{and} \\ \cosh K_T l \cdot \cos K_T l - 1 = 0 \end{array} \right\} \quad (6)$$

The functions  $W_T$  (and their derivatives),  $\sigma_T$  and  $K_T l$  are tabulated by Bishop and Johnson (1956).

### 2.1.2. Rayleigh (Energy) Method

The exact solution of the differential equation of motion of a more complicated system is not always possible. In such a case an approximate value for a natural frequency can be obtained by using the method of Rayleigh.

The strain energy stored in the vibrating beam can be written as

$$U = \frac{EI}{2} \int_0^l \left( \frac{\partial^2 w}{\partial x^2} \right)^2 dx$$

$$= \sin^2 \omega_T t \cdot \frac{EI}{2} \int_0^l \left( \frac{d^2 W_T}{dx^2} \right)^2 dx$$

for  $w = W_T(x) \cdot \sin \omega_T t$

The kinetic energy of the beam can similarly be written as

$$T = \frac{Ap}{2g} \int_0^l \left( \frac{\partial w}{\partial t} \right)^2 dx$$

$$= \cos^2 \omega_r t \cdot \frac{Ap \omega_r^2}{2g} \int_0^l W_r^2 dx$$

Also,  $U + T = \text{CONSTANT} = U_{\text{max.}} = T_{\text{max.}}$

Therefore, equating maximum strain and kinetic energies

$$\frac{Ap \omega_r^2}{2g} \int_0^l W_r^2 dx = \frac{EI}{2} \int_0^l \left( \frac{d^2 W_r}{dx^2} \right)^2 dx$$

$$\omega_r^2 = \frac{EIg}{Ap} \cdot \frac{\int_0^l \left( \frac{d^2 W_r}{dx^2} \right)^2 dx}{\int_0^l W_r^2 dx} \quad (7)$$

If  $W_r$  in this equation is the exact form which satisfies the equation of motion and the boundary conditions, then  $\omega_r$  is the exact frequency.

Rayleigh's method is to assume an approximate shape for  $W$  which satisfies at least the geometrical boundary conditions at the ends of the beam. It can be shown that the estimate of  $\omega_r$  obtained by this method is always greater than the exact value.

As an illustration take the case of a uniform cantilever beam with boundary conditions

$$\left. \begin{aligned} W_r = \frac{dW_r}{dx} = 0 \quad \text{at} \quad x = 0 \\ \frac{d^2 W_r}{dx^2} = \frac{d^3 W_r}{dx^3} = 0 \quad \text{at} \quad x = l \end{aligned} \right\}$$



For the lowest natural frequency we will take for  $W_1$  the expression for static deflection of the beam under its own weight. This shape satisfies all four of the above conditions and is

$$W_1 = Kx^2(x^2 - 4lx + 6l^2)$$

where  $K$  is a constant.

On substituting for  $W_1$  in the energy integrals we have

$$U_{\max} = \frac{EI}{2} \int_0^l \left( \frac{d^2 W_1}{dx^2} \right)^2 dx = \frac{72}{5} EI K^2 l^5$$

$$T_{\max} = \frac{A\rho\omega_1^2}{2g} \int_0^l W_1^2 dx = \frac{52}{45} \frac{A\rho\omega_1^2}{g} K^2 l^9$$

$$\text{Hence } \omega_1^2 = \frac{EIg}{A\rho l^4} \cdot \frac{72 \times 45}{5 \times 52} = 12.46 \frac{EIg}{A\rho l^4}$$

The exact value from the frequency equation (5) is

$$\omega_1^2 = 12.36236 \dots \frac{EIg}{A\rho l^4}$$

The error in the approximate frequency is thus less than 1% showing that this method of approximating a natural frequency can yield a satisfactory result.

## 2.2. Rectangular Cantilever Plates.

### 2.2.1. The Plate Equation of Motion.

In the case of a beam the length is very much greater than the breadth so that the beam can be treated as one-dimensional i.e. Deflection  $w$  or  $W_x$  is dependent on only one space variable,  $x$ . For a plate the breadth is comparable with the length and  $W_x$  becomes a function of two space coordinates,  $x$  and  $y$ .

Corresponding to equation (1) for a uniform beam we have, from the theory of thin plates of uniform thickness, the plate equation

$$D \left\{ \frac{\partial^4 w}{\partial x^4} + 2 \frac{\partial^4 w}{\partial x^2 \partial y^2} + \frac{\partial^4 w}{\partial y^4} \right\} + \frac{\rho h}{f} \frac{\partial^2 w}{\partial t^2} = 0$$

or

$$\nabla^4 w + \frac{\rho h}{f D} \frac{\partial^2 w}{\partial t^2} = 0 \quad (8)$$

The boundary conditions to be satisfied by  $w$  at the edges of the plate, Fig. 1, are in general more complicated than those for a beam.

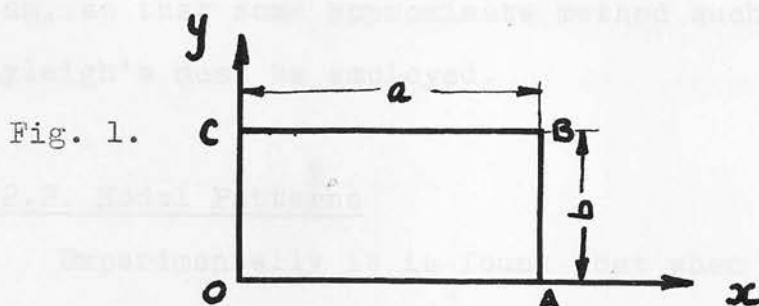


Fig. 1.

For a cantilever plate clamped at CO and free at the other three edges, the boundary conditions are (Timoshenko 1940):

$$\left. \begin{aligned} \text{On CO : } [w]_{x=0} &= \left[ \frac{\partial w}{\partial x} \right]_{x=0} = 0 \\ \text{OA : } \left[ \frac{\partial^2 w}{\partial y^2} + \nu \frac{\partial^2 w}{\partial x^2} \right]_{y=0} &= \left[ \frac{\partial^3 w}{\partial y^3} + (2-\nu) \frac{\partial^3 w}{\partial y \partial x^2} \right]_{y=0} = 0 \\ \text{AB : } \left[ \frac{\partial^2 w}{\partial x^2} + \nu \frac{\partial^2 w}{\partial y^2} \right]_{x=a} &= \left[ \frac{\partial^3 w}{\partial x^3} + (2-\nu) \frac{\partial^3 w}{\partial x \partial y^2} \right]_{x=a} = 0 \\ \text{BC : } \left[ \frac{\partial^2 w}{\partial y^2} + \nu \frac{\partial^2 w}{\partial x^2} \right]_{y=b} &= \left[ \frac{\partial^3 w}{\partial y^3} + (2-\nu) \frac{\partial^3 w}{\partial y \partial x^2} \right]_{y=b} = 0 \end{aligned} \right\} \quad (9)$$

At the free corners,

$$\begin{aligned} \text{A : } \left[ \frac{\partial^2 w}{\partial x \partial y} \right]_{x=a, y=0} &= 0 \\ \text{B : } \left[ \frac{\partial^2 w}{\partial x \partial y} \right]_{x=a, y=b} &= 0 \end{aligned}$$

For harmonic motion the solution of equation (8) might be written in the form

$$w(x, y, t) = W_T(x, y) \cdot A_T \sin \omega_T t \quad (10)$$

where  $W_r(x,y)$  is a dimensionless normal-mode function denoting the shape of the vibration form at the  $r^{\text{th}}$  natural frequency  $\omega_r$ , and  $A_r$  has the dimension of length. Thus,

$$\nabla^2 W_r - \frac{\rho h}{gD} \omega_r^2 W_r = 0 \quad (11)$$

It is <sup>NOT</sup> possible to solve this equation exactly for  $W_r$  and  $\omega_r$  as in the case of the vibrating beam, so that some approximate method such as Rayleigh's must be employed.

### 2.2.2. Nodal Patterns

Experimentally it is found that when a plate vibrates at a natural frequency the zeros of  $W_r$  form a stationary pattern of lines which are approximately parallel to the sides of the plate. Since, in general, each frequency  $\omega_r$  is associated with a particular function  $W_r$  each pattern of "nodal lines" corresponds to a definite frequency. The patterns can be found experimentally by sprinkling sand, or a similar substance, on to the vibrating plate. Provided that the amplitude of vibration is great enough to produce accelerations of more than one "g", the sand will tend to collect at the zeros of  $W_r$ .

### 2.2.3. Rayleigh Method

Assuming that the nodal lines are parallel to the sides of the plate, G.B. Warburton (1954) takes

the deflection in the form

$$w = W(x,y) \cdot \sin \omega t = A \cdot \theta_m(x) \cdot \phi_n(y) \cdot \sin \omega t \quad (12)$$

where  $\theta_m(x)$  and  $\phi_n(y)$  are the beam functions for cantilever and free-free beams respectively.

These are defined by equations (5) and (6) where  $x$  is replaced by  $y$  in (6), and the length  $l$  is replaced by  $a$  in equation (5) and  $b$  in equation (6).

A mode of vibration is identified with the number of zeros  $m$  of  $\theta_m(x)$  and  $n$  of  $\phi_n(y)$ . For example, Fig. 2. shows the mode  $mn$ , where  $m = 3$  and  $n = 2$ .

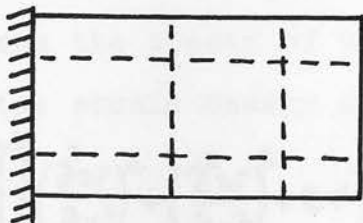


Fig. 2. Nodal Pattern

$$m = 3; n = 2.$$

The lowest mode of vibration of a free-free beam is that corresponding to  $n = 2$  so that functions  $\phi_0(y)$  and  $\phi_1(y)$  have yet to be defined. These functions are taken to represent rigid-body translation and rotation respectively.

That is,

$$\left. \begin{aligned} \theta_m(x) &= (\cosh K_m x - \cos K_m x) - \sigma_m (\sinh K_m x - \sin K_m x) \\ \text{with} \\ \sigma_m &= \frac{\sinh K_m a - \sin K_m a}{\cosh K_m a + \cos K_m a} \\ \text{and} \\ \cosh K_m a \cdot \cos K_m a + 1 &= 0 \\ m &= 1, 2, 3, \dots \end{aligned} \right\} (13)$$

$$\phi_0(y) = 1$$

$$\phi_1(y) = \sqrt{3} \left(1 - \frac{2y}{b}\right)$$

$$\phi_n(y) = (\cosh K_n y + \cos K_n y) - \sigma_n (\sinh K_n y + \sin K_n y)$$

$$n = 2, 3, 4, \dots$$

with

$$\sigma_n = \frac{\cosh K_n b - \cos K_n b}{\sinh K_n b - \sin K_n b}$$

and

$$\cosh K_n b \cdot \cos K_n b - 1 = 0$$

(14)

The above functions satisfy the geometrical boundary conditions of zero slope and deflection at  $x = 0$ , but in general do not satisfy the other conditions in equation (9).

From the theory of thin plates (Timoshenko 1940) the strain energy due to bending is given by

$$U = \frac{D}{2} \iint_0^a \int_0^b \left\{ \left( \frac{\partial^2 w}{\partial x^2} \right)^2 + \left( \frac{\partial^2 w}{\partial y^2} \right)^2 + 2\nu \frac{\partial^2 w}{\partial x^2} \frac{\partial^2 w}{\partial y^2} + 2(1-\nu) \left( \frac{\partial^2 w}{\partial x \partial y} \right)^2 \right\} dx dy$$

and kinetic energy

$$T = \frac{\rho h}{2g} \iint_0^a \int_0^b \left( \frac{\partial w}{\partial t} \right)^2 dx dy$$

Therefore

$$U_{\max.} = \frac{D}{2} \iint_0^a \int_0^b \left\{ \left( \frac{\partial^2 W}{\partial x^2} \right)^2 + \left( \frac{\partial^2 W}{\partial y^2} \right)^2 + 2\nu \frac{\partial^2 W}{\partial x^2} \frac{\partial^2 W}{\partial y^2} + 2(1-\nu) \left( \frac{\partial^2 W}{\partial x \partial y} \right)^2 \right\} dx dy \quad (15)$$

$$T_{\max.} = \frac{\rho h}{2g} \omega^2 \iint_0^a \int_0^b W^2 dx dy \quad (16)$$

whence

$$\omega^2 = \frac{U_{\max.}}{\frac{\rho h}{2g} \iint_0^a \int_0^b W^2 dx dy} \quad (17)$$

Warburton then substitutes for  $W$  from equations (12), (13) and (14). He defines a non-dimensional frequency factor  $\lambda$  by



$m$	$G_x$	$H_x$	$J_x$	$n$	$G_y$	$H_y$	$J_y$
				0	0	0	0
1	0.597	-0.0870	0.471	1	0	0	$\frac{12}{\pi^2}$
2	1.494	1.347	3.284	2	1.506	1.248	5.017
3, 4, ...	$(m-\frac{1}{2})$	$(m-\frac{1}{2})^2 \left[ 1 - \frac{2}{(m-\frac{1}{2})\pi} \right]$	$(m-\frac{1}{2})^2 \left[ 1 + \frac{2}{(m-\frac{1}{2})\pi} \right]$	3, 4, ...	$(n-\frac{1}{2})$	$(n-\frac{1}{2})^2 \left[ 1 - \frac{2}{(n-\frac{1}{2})\pi} \right]$	$(n-\frac{1}{2})^2 \left[ 1 + \frac{2}{(n-\frac{1}{2})\pi} \right]$

TABLE 1.

$$\lambda^2 = \frac{\rho h a^4}{g D \pi^4} \cdot (2 \pi f)^2 \quad (18)$$

where  $\omega^2 = (2 \pi f)^2$  and from the substitution for  $W$  in (17) it is shown that (17) can also be written as

$$\lambda^2 = G_x^4 + G_y^4 \left(\frac{a}{b}\right)^4 + 2 \left(\frac{a}{b}\right)^2 [v H_x H_y + (1-v) J_x J_y] \quad (19)$$

The coefficients  $G_x$ ,  $G_y$ ,  $H_x$ ,  $H_y$ ,  $J_x$  and  $J_y$  depend on the nodal pattern and the boundary conditions.

For all combinations of clamped, free and freely-supported edges (fifteen cases in all) Warburton has evaluated and tabulated these coefficients in terms of the assumed nodal pattern of  $m$  and  $n$  nodal lines parallel to the edges of the plate. The values of the coefficients are given in Table 1 for the case of a cantilever plate.

Given the dimensions and elastic constants of a plate it is possible to obtain quickly reasonably accurate values of the natural frequencies by making use of Table 1 and equations (18) and (19). When frequencies obtained by this method are compared with experimental values it appears that the greatest errors arise for modes with  $n = 1$ . This can probably be attributed to the "stiffening" effect of the assumption of linear variation of deflection in the  $y$  - direction. This "stiffening" will increase the strain energy  $U$ , and hence the frequency.



#### 2.2.4. Rayleigh - Ritz Method

A variation of this energy method of calculation of frequencies is one which was used by Rayleigh himself for simple systems, and which was independently developed by Ritz and used by him in his investigation of the natural frequencies and modes of vibration of a square plate with all edges free (Ritz, 1909).

The procedure is based on an assumed form for  $W$  which contains an arbitrary parameter. The frequency expression (17) is then minimised with respect to the parameter thus giving a better approximation to frequency and mode shape than would otherwise be obtained. The frequencies given by this method are greater than the true values.

Young (1950) and Barton (1951) use this so called Rayleigh-Ritz method to obtain frequencies and mode shapes for plates with various edge conditions. They follow Ritz in assuming for  $W$  the series expression

$$W(x,y) = \sum_m \sum_n A_{mn} \theta_m(x) \cdot \phi_n(y) \quad (20)$$

where  $\theta_m(x)$  and  $\phi_n(y)$  are normal mode functions for beams with clamped, free or freely-supported edges.

Equation (20) is substituted in the energy expression for frequency, equation (17), which is then minimised with respect to each of the coefficients  $A_{mn}$ . This is done by differentiating equation (17) with respect to one of the coefficients,

say  $A_{ik}$ , and equating the result to zero.

$$\frac{\partial(\omega^2)}{\partial A_{ik}} = \frac{2g}{\rho h} \frac{(\iint W^2 dx dy) \frac{\partial u_{\max}}{\partial A_{ik}} - u_{\max} \cdot \frac{\partial}{\partial A_{ik}} \iint W^2 dx dy}{(\iint W^2 dx dy)} = 0$$

Or, since

$$u_{\max} = \frac{\rho h}{2g} \omega^2 \iint W^2 dx dy$$

we have for each coefficient an expression of the form,

$$\frac{\partial u_{\max}}{\partial A_{ik}} - \omega^2 \frac{\rho h}{2g} \cdot \frac{\partial}{\partial A_{ik}} \iint_0^a \int_0^b W^2 dx dy = 0 \quad (21)$$

If equation (20) gives  $W$  in terms of an infinite series then equation (21) represents an infinite set of equations in the coefficients  $A_{mn}$ . The condition that (21) represents a consistent set of equations is that the determinant of the coefficients of  $A_{mn}$  must be zero. This leads to an infinite determinant, the roots of which are the natural frequencies of vibration of the plate.

Using an eighteen term series for  $W$  with  $m = 1, 2, 3$ , and  $n = 0, 1, 2, 3, 4, 5$ , Young evaluates frequencies and coefficients  $A_{mn}$  by using an iterative procedure to solve the set of equations. This is for a square cantilever plate. i.e.  $a = b$ . Since any natural mode of vibration will either be symmetrical or anti-symmetrical about the line  $y = \frac{b}{2}$ , it is found that the set of eighteen equations separates into two independent groups of nine equations containing either those coefficients for which  $n$  is odd or those for which  $n$  is even. Tabulated values of  $A_{mn}$ , for  $m = 1, 2, 3$ , and  $n = 1, 3, 5$  or  $0, 2, 4$ , and values of frequency  $\omega$  are

given for the first five modes of a square cantilever plate. Similar tables are presented for a square plate clamped on all edges (6 modes from 36 term series), and for a square plate clamped on two adjacent edges and free on the other two (5 modes from 9 term series).

In carrying out the integration and differentiation in equation (21) it is necessary to evaluate certain integrals of the beam

functions  $\theta_m(x)$  and  $\phi_n(y)$ . The set of functions  $\theta_m(x)$  [or  $\phi_n(y)$ ] are orthogonal in the region  $0 \leq x \leq a$  [ $0 \leq y \leq b$ ].

i.e

$$\left. \begin{aligned} \int_0^a \theta_r \cdot \theta_s \cdot dx &= a \quad \text{for } r=s \\ &= 0 \quad \text{for } r \neq s \end{aligned} \right\} (22)$$

$$\left. \begin{aligned} \int_0^b \phi_p \cdot \phi_q \cdot dy &= b \quad \text{for } p=q \\ &= 0 \quad \text{for } p \neq q \end{aligned} \right\}$$

also

$$\left. \begin{aligned} \int_0^a \frac{d^2 \theta_r}{dx^2} \cdot \frac{d^2 \theta_s}{dx^2} \cdot dx &= a \cdot \frac{(K_r a)^4}{a^4} \quad \text{for } r=s \\ &= 0 \quad \text{for } r \neq s \end{aligned} \right\} (23)$$

$$\left. \begin{aligned} \int_0^b \frac{d^2 \phi_p}{dy^2} \cdot \frac{d^2 \phi_q}{dy^2} \cdot dy &= b \cdot \frac{(K_p b)^4}{b^4} \quad \text{for } p=q \\ &= 0 \quad \text{for } p \neq q \end{aligned} \right\}$$

Provided that we arbitrarily define  $K_0 = K_1 = 0$

for  $\phi_0$  and  $\phi_1$  since

$$\int_0^b \left( \frac{d^2 \phi_0}{dy^2} \right)^2 dy = \int_0^b \left( \frac{d^2 \phi_1}{dy^2} \right)^2 dy = 0$$

Values are also required of the integrals,

$$\int_0^a \theta_r \cdot \frac{d^2 \theta_s}{dx^2} \cdot dx, \quad \int_0^a \frac{d\theta_r}{dx} \cdot \frac{d\theta_s}{dx} \cdot dx.$$

$$\int_0^b \phi_p \cdot \frac{d^2 \phi_q}{dy^2} \cdot dy, \quad \int_0^b \frac{d\phi_p}{dy} \cdot \frac{d\phi_q}{dy} \cdot dy.$$

These are tabulated by Young for clamped-clamped, clamped-free and free-free functions. Values are also given of other quantities which arise in the analysis.

The use of beam functions in the series for  $W$  has the advantage that terms in the leading diagonal of the determinant become large compared with the others, thus improving the convergence of the iterative procedure.

The work of Young is extended by Barton who treats rectangular plates as a special case of skew or oblique plates. i.e. Plates in which the sides of length "a" are not at right angles to the clamped edge. (cantilever Plates). The procedure followed by Young is again used to obtain a set of equations in the coefficients  $A_{mn}$  and numerical calculations are made for rectangular cantilever plates with length to breadth ratios  $\frac{a}{b} = \frac{1}{2}, 1, 2, 5$  using an eighteen term series for deflection. The resultant coefficients  $A_{mn}$  and their associated frequency have been tabulated for the first three symmetrical modes and for the first two anti-symmetrical modes.

From these calculated values of frequencies a graph has been drawn showing the variation of

frequency of each mode with length - to - breadth ratio. Within the range of length - to - breadth ratios used by Barton and Young and for the modes they consider, it is a simple matter to obtain the required frequency by examining the graph. The modes of vibration are obtained from equation (20) and the tabulated values of  $A_{mn}$ . For other modes of vibration or for length - to - breadth ratios outwith the range considered it is necessary to repeat the whole analysis, including the solution of a large number of simultaneous equations.

#### 2.2.5. The Variational Method.

In appendix 1 it is shown that if calculus of Variations is applied directly to minimise equation (17) then  $W$  must satisfy the differential equation (11) and also the boundary conditions at the edges of the plate. Since the differential equation cannot be solved no useful information has been gained. However, Martin (1956) has applied variational methods to the solution of the problem of vibration of a cantilever plate by first making an assumption as to the general form of the function  $W$ . Thus, as an approximation

$$W = \theta(x) \cdot \phi(y)$$

where  $\phi(y)$  is taken as one of the free-free beam functions and  $\theta(x)$  represents a function which can be varied with the boundary conditions

$$\theta(0) = \frac{d\theta(0)}{dx} = 0$$

When the required variation is carried out  $\phi(y)$  is considered constant and  $\theta(x)$  is subject to the above boundary conditions. This procedure leads to an ordinary differential equation for  $\theta(x)$  and to two boundary conditions for  $\theta(x)$  at  $x = a$ .

The solution of the differential equation is reasonably simple, but it leads to a complicated equation for frequency which Martin solves graphically by plotting length-to-breadth ratio against frequency for each mode of vibration.

For those modes of vibration with no nodal lines perpendicular to the clamped edge the methods of Warburton and Martin give exactly the same answer for frequency. That is

$$\omega^2 = \frac{gD}{\rho R} \cdot \left(\frac{\pi}{a}\right)^4 \cdot \left(m - \frac{1}{2}\right)^4$$

where  $m$  is a positive integer. This is the same expression as is obtained for a cantilever beam vibrating in the same mode but with  $\frac{D}{R}$  replacing  $\frac{EI}{A}$ .

#### 2.2.6. The Finite-difference Approach.

The methods so far discussed for calculation of natural frequencies yield approximate values which are higher than the exact frequencies. By replacing the differential equation (11) by its corresponding difference equation, approximate values for frequencies are obtained which are lower than the exact values. This method has been used by D. Williams (1957) to obtain the fundamental

frequency of vibration of a square plate simply supported on each edge, Fig. 3., the exact solution for which is

$$\omega_1 = \frac{2\pi^2}{a^2} \sqrt{\frac{gD}{\rho h}}$$

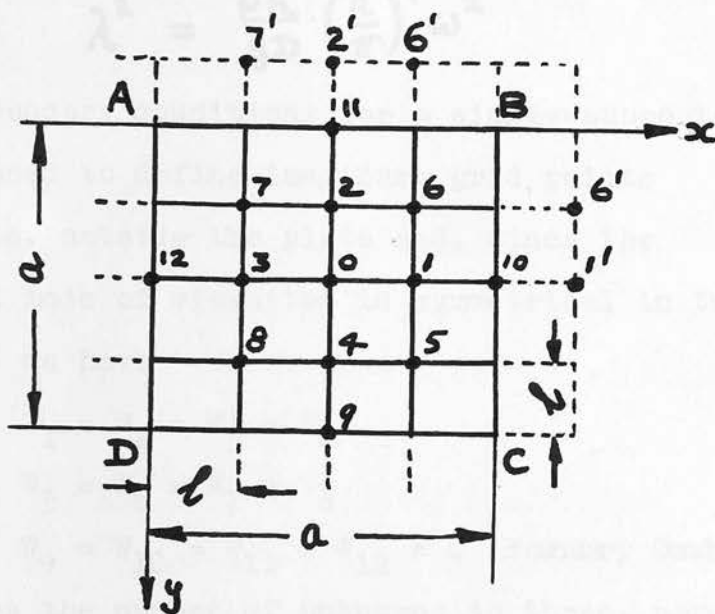


Fig. 3.

A rectangular grid of mesh length  $l$  is drawn on the plate ABCD. For a first approximation  $l$  has been taken as one quarter of the length of a side.

i.e.  $l = \frac{a}{4}$ .

For a point 0 surrounded by a pattern of twelve points as shown in Fig. 3. we can use central difference formulae to transform the differential equation (11) into

$$\frac{1}{l^4} \left[ 20W_0 - 8 \sum_{r=1}^4 W_r + 2 \sum_{r=5}^8 W_r + \sum_{r=9}^{12} W_r \right] - \frac{\rho h}{gD} \cdot \omega^2 W_0 = 0$$

or

$$\left[ 20 - \left( \frac{\pi}{4} \right)^4 \lambda^2 \right] W_0 - 8 \sum_{r=1}^4 W_r + 2 \sum_{r=5}^8 W_r + \sum_{r=9}^{12} W_r = 0 \quad (24)$$

where  $W_0$  is the deflection at point 0, etc.

$$\left(\frac{\pi}{4}\right)^4 \lambda^2 = \frac{\rho h}{gD} \cdot \omega^2 l^4 = \frac{\rho h}{gD} \cdot \omega^2 \cdot \left(\frac{a}{4}\right)^4$$

and, as before

$$\lambda^2 = \frac{\rho h}{gD} \cdot \left(\frac{a}{\pi}\right)^4 \cdot \omega^2$$

The boundary conditions for a simply-supported plate are used to define imaginary grid points  $1', 2', 6'$  etc. outside the plate and, since the fundamental mode of vibration is symmetrical in two directions, we have

$$W_1 = W_2 = W_3 = W_4$$

$$W_5 = W_6 = W_7 = W_8$$

with  $W_9 = W_{10} = W_{11} = W_{12} = 0$  (Boundary Condition)

This reduces the number of unknowns to three, namely

$$W_0, W_1, W_6.$$

Application of equation (24) to each of the points 0, 1, 6 leads to three algebraic equations in  $W_0, W_1$  and  $W_6$  and thence to the frequency equation

$$\left(\frac{\pi^2 \lambda}{16}\right)^6 - 64 \left(\frac{\pi^2 \lambda}{16}\right)^4 + 832 \left(\frac{\pi^2 \lambda}{16}\right)^2 - 1024 = 0 \quad (25)$$

The lowest root is

$$\frac{\pi^2 \lambda_1}{16} = 1.173$$

Hence

$$\omega_1 = \frac{\pi^2 \lambda_1}{16} \times \frac{16}{a^2} \sqrt{\frac{gD}{\rho h}} = \frac{18.76}{a^2} \sqrt{\frac{gD}{\rho h}}$$

This answer is 5% below the exact value

$$\omega_1 = \frac{2\pi^2}{a^2} \sqrt{\frac{gD}{\rho h}} = \frac{19.76}{a^2} \sqrt{\frac{gD}{\rho h}}$$

The remaining two roots of equation (25)



correspond to approximations to the second and third doubly-symmetric modes but they are 60 -70% below the exact values. A closer grid spacing would yield greater accuracy, but if there are  $n$  unknowns  $n$  simultaneous equations are obtained and hence a frequency equation of the  $n^{\text{th}}$  degree.

In the case of a cantilever plate the boundary conditions are more complicated, and because there is at most one line of symmetry the same grid spacing as in the previous problem will give more unknowns and hence a frequency equation of higher degree.

Livesley and Birchall (1956) use finite differences to study the static deflection of a cantilever plate and give a useful discussion of boundary conditions in finite difference form. They consider that it may be more important to satisfy the condition of zero force at a free corner than to satisfy the vanishing of the third order differential condition of equations (9) on a free edge.

#### 2.2.7. Comparison of the various method of calculating natural frequencies.

To obtain reasonably accurate estimates of the first  $n$  natural frequencies using finite differences, one would require to solve possibly as many as  $n^2$  simultaneous algebraic equations. For hand computation this would, in many cases, be too

laborious to be practicable. Williams, however, suggests that the method is ideal for use with an electronic digital computer since complicated boundary conditions and even variations of sections (thickness of plate, etc.) can be incorporated with little difficulty.

The final step in the procedure used by Barton and Young also requires solution of simultaneous equations, but for the same order of accuracy the number of equations is much smaller than in the finite difference method.

This method reduces to that of Warburton when a single product of beam functions is substituted for  $W$  in place of a series of products. Warburton's analysis has the great advantage of simplicity since the formula for a particular frequency can be evaluated without reference to other frequencies. i.e. No simultaneous equations. It is to be expected that the errors will be larger than in the Barton-Young analysis but this increase is appreciable only for certain modes of vibration, notably those with one nodal line perpendicular to the clamped edge. For these modes a better approximation can be obtained by taking a two-term series for  $W$  of the form

$$W_{mn} = A[\theta_m(x) \cdot \phi_n(y) + B \cdot \theta_r(x) \cdot \phi_s(y)]$$

and minimising  $\omega^2$  in equation (17) with respect to the parameter B. For example, consider the first torsional mode for which

$$\vartheta_m(x) \cdot \phi_n(y) = \vartheta_1(x) \cdot \phi_1(y)$$

and take for the additional term

$$\vartheta_1(x) \cdot \phi_2(y) = \vartheta_2(x) \cdot \phi_1(y)$$

$$\phi_1(y) = \sqrt{3} \cdot \left(1 - \frac{2y}{b}\right)$$

$$\vartheta_m(x) = (\cosh \kappa_m x - \cos \kappa_m x) - \sigma_m (\sinh \kappa_m x - \sin \kappa_m x)$$

$$\kappa_1 a = 1.875 \quad ; \quad \kappa_2 a = 4.694$$

Because of the form of  $\phi_1(y)$  all second derivatives with respect to y vanish and the energy equation (17) for frequency becomes

$$\frac{\omega^2 \rho h}{g D} = \lambda^2 \left(\frac{\pi}{a}\right)^4 = \frac{\int_0^a \int_0^b \left\{ \left(\frac{\partial^2 W}{\partial x^2}\right)^2 + 2(1-\nu) \left(\frac{\partial^2 W}{\partial x \partial y}\right)^2 \right\} dx dy}{\int_0^a \int_0^b W^2 dx dy}$$

The integrals involved can be evaluated by referring to the tables given by Young and we get eventually

$$\lambda^2 \left(\frac{\pi}{a}\right)^4 = \frac{1}{a^4} \cdot \frac{[12.362 + 485.5 B^2 + 24(1-\nu) \left(\frac{a}{b}\right)^2 \{4.648 - 14.74 B + 32.42 B^2\}]}{(1+B^2)}$$

Taking  $\left(\frac{a}{b}\right) = 2$ , and  $\nu = 0.3$ , we have

$$\lambda^2 \pi^4 = \frac{324.36 - 990 B + 2660 B^2}{(1+B^2)}$$

This expression has a minimum value when  $B = 0.205$ , leading to

$$\lambda = 1.52$$

The corresponding figure obtained by using the one term approximation is  $\lambda = 1.825$

and the experimental value given by Barton is

$$\lambda = 1.47$$

The one- and two-term approximations for  $W$  lead to values for the frequency which are respectively 24% and 3.2% higher than the experimental result.

No great improvement is obtained by using more terms in the expression for  $W$ ; the Young-Barton analysis applied to an eighteen-term series yields a value for  $\lambda$  which is 2.8% higher than the experimental result.

There does not seem to be any obvious guide to the best choice of  $\theta_r(x) \cdot \phi_s(y)$ . In any particular case this will probably be most easily decided by trial and error.

Frequencies determined by the procedure developed by Martin are more accurate than those from the one-term approximation but, in general, are less accurate than those from the two-term series. It would appear that this method might be improved (at the expense of an increase in complexity) by variation of the function  $\phi$  instead of  $\theta$ . The use of a cantilever-beam function for  $\theta$  would automatically satisfy the slope and deflection conditions at the clamped edge and the problem would contain conditions for two free edges instead of one. Martin suggests that 'A more difficult enterprise would be to take both  $\theta$  and  $\phi$

CHAPTER III

as two independent variable functions'. This is not profitable in view of the accuracy reported above for the Rayleigh-Ritz method.

In the work which follows some form of the Rayleigh-Ritz method will be used, including the one- or two-term approximation where this is satisfactory.

$\alpha = k P^3 \quad (26)$

where,  $\alpha$  - the change in distance between the centers of the bodies.

$k$  = the force between the bodies

$k$  = a constant for a given pair of bodies, dependent on the elastic constants and radii of curvature at the point of contact.

Hertz (1891) derived this equation by assuming that near the point of contact the surfaces were of the second degree (e.g. spherical) and that elastic deformations were confined to a small region around the point of contact. Neglecting the energy losses due to vibrations, etc., Hertz applied the above equation to the study of the impact of two elastic bodies and obtained an expression for the duration of contact. A later investigation by Boussinesq (1901) showed that for spheres, for example, the duration of contact was much greater than the period of the lowest mode of vibration of the spheres so that vibrations could be neglected.

Hertz's (1891) work is used as a basis in developing a theory for the impact of a sphere

## CHAPTER III

Impact and Transient Vibrations3.1. Historical Introduction

When two elastic bodies are in contact the static force pressing them together is related to the change in distance between their centres by a non-linear algebraic equation. That is,

$$\alpha = k P^{\frac{2}{3}} \quad (26)$$

where,  $\alpha$  = the change in distance between the centres of the bodies.

$P$  = the force between the bodies

$k$  = a constant for a given pair of bodies, dependent on the elastic constants and radii of curvature at the point of contact.

Hertz (1881) derived this equation by assuming that near the point of contact the surfaces were of the second degree (e.g. spherical) and that elastic deformations were confined to a small region around the point of contact. Neglecting the energy losses due to vibrations, etc., Hertz applied the above equation to the study of the impact of two elastic bodies and obtained an expression for the duration of contact. A later investigation by Rayleigh (1906) showed that for spheres, for example, the duration of contact was much greater than the period of the lowest mode of vibration of the spheres so that vibrations could be neglected.

Timoshenko (1913) made use of Hertz's work in developing a theory for the impact of a sphere

on a simply-supported beam. In accounting for vibrations of the beam and deformation at the point of contact, a non-linear integral equation was obtained for the force  $P$ . With the knowledge that  $P$  starts from zero and is never negative, a numerical solution of the equation was obtained by assuming the time  $t$  to be divided into small intervals during which  $P$  could be considered constant. The step-by-step calculation was continued until  $P$  returned to zero. The accuracy of this process depends on the use of a large number of small intervals, so that the calculation can be very tedious and laborious and the result obtained applies only to a particular numerical problem.

Timoshenko also showed theoretically, and was supported by later experimental work of H.L. Mason (1936) and R.N. Arnold (1937), that under certain conditions the impact process was no longer simple but consisted of a series of sub-impacts or multiple blows. This more complicated case appears to arise when the mass of the sphere is not very much smaller than the mass of the object with which it collides. It is not intended to study this case here.

The above numerical method does not readily lend itself to a study of the effect of varying some of the parameters in the impact process, such as the mass of the sphere, its velocity immediately before impact, etc. In investigating this problem

Zener and Feshbach (1939) produced a powerful approximate method for the solution of the simple impact of a sphere on a beam. By equating the total impulse acting on the sphere to the change in its momentum, a "normalised" force was obtained which was quite insensitive to the approximate force-time shapes used in the calculations. If the sphere of mass  $\frac{W}{g}$  has a velocity  $v$  immediately before impact, and a velocity  $ev$  in the opposite direction immediately after impact, we have

$$\int_0^T P \cdot dt = \frac{W}{g} v(1+e) \quad (27)$$

where  $T$  is the duration of contact and  $e$  is a coefficient of restitution. Using the "normalised" force this gives

$$\int_0^T \bar{P} \cdot dt = 1 \quad (28)$$

and

$$\bar{P} = \frac{P}{\frac{W}{g} v(1+e)} \quad (29)$$

By equating the kinetic energy lost by the sphere to the sum of the kinetic and strain energies gained by the beam, Zener and Feshbach were able to calculate the quantity  $e$  within 3% of that obtained from the numerical analysis of Timoshenko.

Using this method with two different "normalised" forces, Lee (1940) showed that the distribution of energy among the various modes of vibration was little affected by the choice of force-time shape. Like Zener and Feshbach he equated the maximum value of the approximate force to that of the Hertz force, so that the contact time  $T$  depended on the



chosen force-time shape.

Eringen (1953) investigated the impact of a sphere on a beam or plate and by suitably defining his symbols treated beams and plates as one problem. The integral equation of Timoshenko was solved approximately using two methods.

(a) Generalised Galerkin method

(b) Collocation method.

An approximate shape was chosen for the force  $P$  containing a number of unknown parameters. In (a) the parameters were evaluated by minimising certain integrals, while in (b) they were determined by satisfying the integral equation at various characteristic points such as the beginning and end of contact and the point of maximum force. Flexural deflections were then found by solving the differential equation of forced vibration of the beam or plate. Eringen suggests that the series for deflections converges rapidly but that the series for stress obtained by differentiation converges only slowly.

Stresses and deflections produced in rectangular plates (with combinations of clamped and simply-supported edges) by dynamic loads were considered by Greenspon (1955). His approach was based on the concept of a dynamic load factor, i.e. The deflection was obtained in the form of a series, each term of which consisted of the static deflection in a particular mode multiplied by a factor which

depended on the load shape. e.g. A unit load applied gradually to a single degree-of-freedom system may produce a deflection  $w$ . It can be shown that the same load applied suddenly (unit step-function) produces a maximum deflection of  $2w$ . The figure 2 in this case is the dynamic load factor. To obtain an estimate of the maximum deflection produced by a given load acting on a plate Greenspon added the first four terms of his series assuming that they were in phase. This will not in general be true and since no experimental results were given the extent of the error is not known. Greenspon states that this calculation should always give maximum deflections or stresses higher than the values obtained by computing the response as a function of time and that the method should be adequate for pulses in which the first mode of vibration makes the primary contribution to the deflection and stress. That the method can produce reasonable results is shown by a comparison of static deflections and stresses with those given in Timonshenko (1940). Maximum error is about 3% for stresses and 2% for deflections.

### 3.2. Vibration of a Plate

#### 3.2.1. Arbitrary Force Distribution

The motion of a plate under the action of a load  $F(x,y,t)$  is given by the differential equation

$$D \left\{ \frac{\partial^4 w}{\partial x^4} + 2 \frac{\partial^4 w}{\partial x^2 \partial y^2} + \frac{\partial^4 w}{\partial y^4} \right\} + \frac{\rho h}{g} \frac{\partial^2 w}{\partial t^2} = F(x, y, t)$$

$$\text{or } \frac{gD}{\rho h} \nabla^4 w + \frac{\partial^2 w}{\partial t^2} = \frac{gF}{\rho h} \quad (30)$$

where  $F$  is the load/unit area and  $D = \frac{E h^3}{12(1-\nu^2)}$  is the flexural stiffness of the plate.

Consider a solution in the form of a series.

$$w(x, y, t) = \sum_{r=1}^{\infty} W_r(x, y) \cdot q_r(t) \quad (31)$$

The subscript  $r$  refers to a particular natural frequency and  $W_r(x, y)$  is the mode shape as defined by equations (10), (12) or (20) of the previous chapter. That is

$$W_r(x, y) = [A_{10} \theta_1(x) \phi_0(y) + A_{11} \theta_1(x) \phi_1(y) + \dots]_r \quad (32)$$

Young has calculated several sets of the coefficients  $A_{mn}$  assuming for the first mode that  $A_{10} = 1.0$ , etc. It is more convenient to divide throughout by  $\sqrt{(\sum A_{mn}^2)_r}$  so that we obtain a set of coefficients which satisfy the condition

$$\left[ \sum A_{mn}^2 \right]_r = 1.0 \quad (33)$$

$W_r(x, y)$  is dimensionless and  $q_r(t)$  is a function of time with the dimension of length.

Substitute equation (31) into (30), multiply by a mode shape function  $W_m(x, y)$  and integrate over the area of the plate

$$\frac{gD}{\rho h} \int_A W_m (\nabla^4 \sum W_r q_r) dA + \int_A W_m \left( \sum W_r \frac{d^2 q_r}{dt^2} \right) dA = \int_A \frac{gF W_m}{\rho h} dA \quad (34)$$

Rayleigh (1945) shows that for any boundary conditions

$$\int_A W_m \cdot W_r \cdot dA = 0 \quad m \neq r$$

Also, from equation (11), we have

$$\nabla^2 W_r = \frac{\rho h}{gD} \cdot \omega_r^2 W_r$$

So that

$$\int_A W_m \cdot \nabla^2 W_r \cdot dA = \frac{\rho h}{gD} \cdot \omega_r^2 \int_A W_m \cdot W_r \cdot dA = 0 \quad m \neq r$$

Equation (34) then reduces to

$$\frac{gD}{\rho h} \int_A W_m \cdot \nabla^2 W_m \cdot z_m \cdot dA + \int_A W_m^2 \cdot \frac{d^2 z_m}{dt^2} \cdot dA = \int_A \frac{g F \cdot W_m}{\rho h} \cdot dA$$

Or

$$\frac{d^2 z_m}{dt^2} + \frac{gD}{\rho h} \cdot \frac{\int_A W_m \cdot \nabla^2 W_m \cdot dA}{\int_A W_m^2 \cdot dA} \cdot z_m = \frac{g}{\rho h} \cdot \frac{\int_A F \cdot W_m \cdot dA}{\int_A W_m^2 \cdot dA}$$

$$\frac{d^2 z_m}{dt^2} + \omega_m^2 \cdot z_m = \frac{g}{\rho h} \cdot \frac{\int_A F \cdot W_m \cdot dA}{\int_A W_m^2 \cdot dA} \quad (35)$$

where the frequency of the  $m^{\text{th}}$  mode of vibration is

$$\omega_m = \sqrt{\frac{gD}{\rho h} \left[ \frac{\int_A W_m \cdot \nabla^2 W_m \cdot dA}{\int_A W_m^2 \cdot dA} \right]} \text{ radians/sec.} \quad (39)$$

### 3.2.2. Force concentrated at a Point

We have

$$\int_A W_m^2 dA = \int_0^a \int_0^b [A_1 \theta_1(\omega) \phi_1(y) + \dots]_m^2 dx dy$$

$$= ab$$

Also, if the loading consists of a concentrated force  $P(t)$  applied at the point whose coordinates

are  $(x_0, y_0)$

$$\int_A F \cdot W_m \cdot dA = P(t) \cdot W_m(x_0, y_0)$$

Equation (35) can therefore be rewritten as

$$\frac{d^2 q_m}{dt^2} + \omega_m^2 q_m = \frac{g \cdot P(t)}{\rho h a b} \cdot W_m(x_0, y_0) \quad (36)$$

If the plate is assumed to start from rest in a position of zero displacement the general solution of equation (36) is of the form

$$q_m(t) = \frac{g}{\rho h a b} \cdot \frac{W_m(x_0, y_0)}{\omega_m} \int_0^t P(\tau) \cdot \sin \omega_m(t - \tau) \cdot d\tau \quad (37)$$

Substitution for  $q_m(t)$  in equation (31) gives the solution for the displacement of any point of the plate under the action of the force  $P(t)$ .

$$w(x, y, t) = \frac{g}{\rho h a b} \sum_{m=1}^{\infty} \frac{W_m(x_0, y_0) \cdot W_m(x, y)}{\omega_m} \int_0^t P(\tau) \cdot \sin \omega_m(t - \tau) \cdot d\tau \quad (38)$$

If, further, we take

$$P(t) = P \cdot \sin \omega t$$

where  $P$  is a constant and  $\omega \neq \omega_m$  the integral can be evaluated directly to give

$$w(x, y, t) = \frac{P g}{\rho h a b} \sum \frac{W_m(x_0, y_0) \cdot W_m(x, y)}{\omega_m^2} \cdot \left[ \frac{\left(\frac{\omega_m}{\omega}\right) \sin \omega t - \left(\frac{\omega_m^2}{\omega}\right) \sin \omega t}{1 - \left(\frac{\omega_m}{\omega}\right)^2} \right] \quad (39)$$

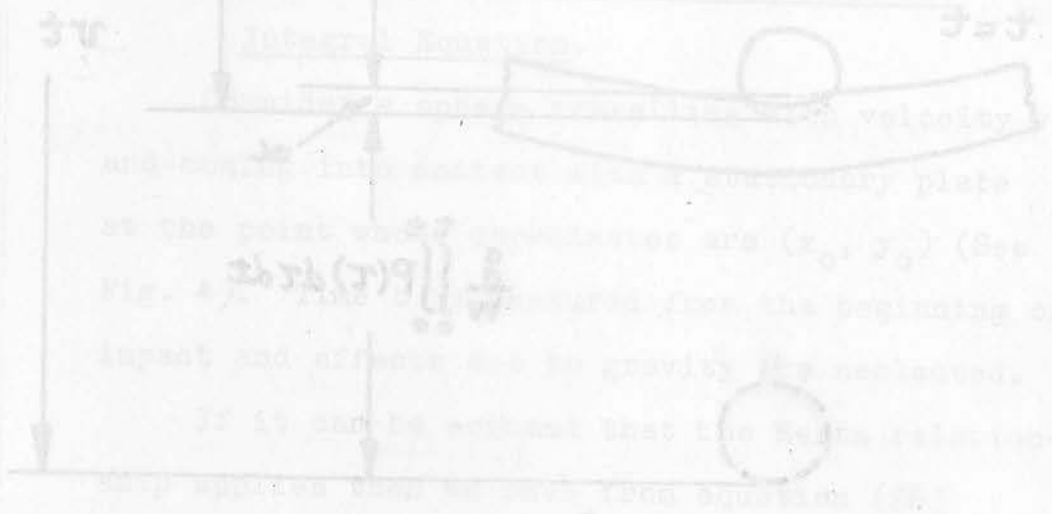
After a time  $T$  where  $T = \frac{\pi}{\omega}$ , the force  $P(t)$  is removed and free vibration of the plate ensues. To find an expression for this we substitute  $T$  for the upper limit in the integral. This is equivalent to putting

$$\begin{aligned} P(\tau) &= P \cdot \sin \omega \tau & 0 < \tau < T \\ &= 0 & T < \tau \end{aligned}$$

On entering out the  $(x_0, y_0)$   $v = 0$

$$w(x, y, t) = \frac{2 \rho_0 \int_{-\infty}^{\infty} \int_{-\infty}^{\infty} \frac{f(x_0, y_0) \sqrt{(x-x_0)^2 + (y-y_0)^2}}{[1 - (\frac{z}{c})^2]} dt - \frac{T}{2} \quad (40)$$

3.2.3. Effect of a Sphere on the Flow - The



and velocity profiles are shown in the figure. The velocity profiles are shown in the figure. The velocity profiles are shown in the figure. The velocity profiles are shown in the figure.

$$\alpha = k P^2(t) \quad (25a)$$

In a time  $t$ , the sphere is displaced a distance  $z$  and the velocity is  $v$ . The velocity is  $v$ . The velocity is  $v$ . The velocity is  $v$ .

$$v = \frac{dz}{dt} = \frac{2 \rho_0 \int_{-\infty}^{\infty} \int_{-\infty}^{\infty} \frac{f(x_0, y_0) \sqrt{(x-x_0)^2 + (y-y_0)^2}}{[1 - (\frac{z}{c})^2]} dt - \frac{T}{2}$$

where  $\frac{dz}{dt}$  is the velocity of the sphere. The velocity is  $v$ . The velocity is  $v$ . The velocity is  $v$ . The velocity is  $v$ .

DEVELOPMENT OF THE THEORY OF BOUNDARY



On carrying out the integration we have

$$w(x,y,t) = \frac{2Pg}{\rho h a b} \int \frac{W_m(x_0, y_0) \cdot W_m(x, y)}{\omega_m^2} \cdot \frac{\left(\frac{\omega_m}{\omega}\right)}{\left[1 - \left(\frac{\omega_m}{\omega}\right)^2\right]} \cdot \cos \frac{\omega_m T}{2} \cdot \sin \omega_m \left(t - \frac{T}{2}\right) \quad (40)$$

### 3.2.3. Impact of a Sphere on the Plate :- The Integral Equation.

Consider a sphere travelling with velocity  $v$  and coming into contact with a stationary plate at the point whose coordinates are  $(x_0, y_0)$  (See Fig. 4). Time  $t$  is measured from the beginning of impact and effects due to gravity are neglected.

If it can be assumed that the Hertz relationship applies then we have from equation (26)

$$\alpha = k P^{\frac{2}{3}}(t) \quad (26a)$$

In a time  $t$ , travelling in unrestrained motion with velocity  $v$ , the sphere will move through a distance

$$vt$$

Due to the existence of the force  $P(t)$  a change in velocity is produced in the sphere, given by

$$-\frac{g}{w} \int_0^t P(\tau) \cdot d\tau$$

where  $\frac{w}{g}$  is the mass of the sphere. This change in the velocity of the sphere leads to a reduction in the distance travelled by the sphere, equal to

$$-\frac{g}{w} \int_0^t \int_0^t P(\tau) \cdot d\tau dt$$



Thus we have for the actual distance transversed by the centre of the sphere

$$S = vt - \frac{g}{W} \int_0^t \int_0^t P(\tau) d\tau dt \quad (41)$$

The deflection of the centre line of the plate at the position  $(x_0, y_0)$  is obtained from equation (38) as

$$w(x_0, y_0, t) = \frac{g}{\rho h a b} \sum \frac{W_m^2(x_0, y_0)}{\omega_m} \int_0^t P(\tau) \sin \omega_m (t - \tau) d\tau \quad (42)$$

Also, by definition,

$$S = \alpha + w(x_0, y_0, t)$$

Substitution from equations (26a), (41) and (42) leads to the integral equation for the force  $P(t)$ .

$$\begin{aligned} vt - \frac{g}{W} \int_0^t \int_0^t P(\tau) d\tau dt \\ = R P^{\frac{2}{3}}(t) + \frac{g}{\rho h a b} \sum \frac{W_m^2(x_0, y_0)}{\omega_m} \int_0^t P(\tau) \sin \omega_m (t - \tau) d\tau \end{aligned} \quad (43)$$

Equation (43) is exactly analogous to that obtained by Timoshenko for the analysis of the impact of a sphere on a simply-supported beam and could be solved, in any particular case, by the numerical procedure used by Timoshenko.

Eringen obtains a similar equation and, after expressing it in non-dimensional form, solves it by approximate methods for the particular cases of two beams, a circular plate, a square plate and a rectangular plate, all simply-supported at the boundaries.

### 3.2.4. An Approximate Solution of the Impact Problem

Instead of attempting to solve equation (43) the approximate method of Zener and Feshbach will be employed to obtain a suitable shape for  $P(t)$  which will then be substituted in equation (40).

Equation (28) which defines the "normalised" force  $\bar{P}(t)$ , is satisfied by

$$\bar{P}(t) = \frac{\pi}{2T} \sin \frac{\pi t}{T} \quad (44)$$

Hence, from equation (29), we have

$$P(t) = \frac{W}{g} v(1+e) \frac{\pi}{2T} \sin \frac{\pi t}{T} \quad (45)$$

Thus in equation (40) we have

$$\omega = \frac{\pi}{T}$$

and

$$P = \frac{W}{g} v(1+e) \frac{\pi}{2T}$$

leading to

$$w(x,y,t) = \frac{Wv(1+e)\pi}{\rho h a b T} \sum \frac{W_m(x_0, y_0) \cdot W_m(x, y)}{\omega_m^2} \cdot \frac{\left(\frac{\omega_m T}{\pi}\right) \cos \frac{\omega_m T}{2}}{\left[1 - \left(\frac{\omega_m T}{\pi}\right)^2\right]} \cdot \sin \omega_m \left(t - \frac{T}{2}\right) \quad (46)$$

The "time of contact",  $T$  in equation (44), is as yet undefined. To find this the amplitude of the normalised force will be equated to the maximum value of the normalised Hertz force.

By considering the changes of momentum occurring during the impact of two elastic spheres it is possible to produce an equation for the Hertz time of contact,  $T_H$  (See, for instance, Timoshenko, 1951). This procedure neglects vibrations, etc. so

that a sphere of weight  $W$  falling with velocity  $v$  on to a fixed solid has a value of unity for the coefficient of restitution. Thus from equation

$$(27) \quad \int_0^{T_H} P_H \cdot dt = \frac{2Wv}{g}$$

Using the subscript  $M$  to denote maximum values we have from Timoshenko (1951)

$$\frac{2Wv}{g} = \frac{8}{5} \cdot \frac{k P_{HM}^{5/3}}{v}$$

$$\text{Also, } T_H = \frac{2.94328 \cdot k P_{HM}^{2/3}}{v}$$

Hence the maximum normalised Hertz force

$$\begin{aligned} \bar{P}_{HM} &= \frac{P_{HM}}{\int_0^{T_H} P_H \cdot dt} = \frac{P_{HM}}{\left(\frac{8}{5} \cdot \frac{k P_{HM}^{5/3}}{v}\right)} \\ &= \frac{5}{8} \times \frac{2.94328 \dots}{T_H} \\ &= \frac{1.83955}{T_H} \end{aligned}$$

Equating this to the maximum value of the approximate normalised force gives

$$\frac{\pi}{2T} = \frac{1.83955}{T_H}$$

Hence,

$$T = 0.854 T_H$$

$$= 3.23 \left[ \frac{\left(\frac{W}{g}\right)^2 (1-v^2)^2}{v E^2 R} \right]^{1/5} \quad (47)$$

Where

$W$  = weight of the sphere

$g$  = acceleration due to gravity

$v$  = velocity of sphere immediately  
before impact

$R$  = radius of the sphere

$E$  = Young's modulus of elasticity for  
the material of the sphere and of  
the plate.

$\nu$  = Poisson's ratio for material of  
sphere and plate.

It is also of interest to calculate the strain at the surface of the plate during free vibration. Strain in the  $x$  - direction is related to the deflection by the equation

$$\begin{aligned} \epsilon_x &= \frac{h}{2} \cdot \frac{\partial^2 w(x,y,t)}{\partial x^2} \quad \text{at the surface of the plate} \\ &= \frac{h}{2} \cdot \frac{Wv(1+e)\pi}{\rho h a b T} \sum \frac{W_m(k,y_0) \cdot \frac{\partial^2 W_m(x,y)}{\partial x^2} \left(\frac{\omega_m T}{\pi}\right) \cos \frac{\omega_m T}{2}}{\omega_m^2 \left[1 - \left(\frac{\omega_m T}{\pi}\right)^2\right]} \sin \omega_m \left(t - \frac{T}{2}\right) \quad (48) \end{aligned}$$

Using the first few terms of the series (46) and (48) deflection and strain histories have been calculated for particular points on the plate. These results will later be compared with those obtained experimentally.

For the case of elastic impact of a sphere on a simply-supported beam Zener and Feshbach obtained a value for the coefficient of restitution  $e$  by equating the kinetic energy lost by the sphere to the sum of the kinetic and strain energies gained by the beam. This method has not been used in the



## CHAPTER 4

### Experiments and Calculations

#### 4.1. The Plate and Clamping Device

Fig. 5. shows the arrangement which was finally adopted for clamping of the fixed edge of the cantilever plate. The thick metal blocks were used to provide a rigid structure which would resist any movement of the plate over the clamped area. This resistance to movement was not obtained when less thick clamping blocks were used. One row of  $\frac{1}{2}$ " diameter Whitworth studs was placed as close as possible to the clamped edge, again in an attempt to minimise movement and to increase the effective stiffness of the support. A further row of studs was used to reduce the possibility that the first row might tend to act as a simple support. The complete unit was then clamped as shown in the diagram to an existing set-up of I-section beams fixed in a concrete base.

#### 4.2. Determination of Natural Frequencies

A block diagram of the apparatus used to determine the natural frequencies of transverse vibration of the plate is shown in Fig. 6.

The method employed was essentially that of finding the frequencies at which the plate would resonate in forced vibration.

The plate was vibrated by an electromechanical vibration-generator which was supplied by an oscillator with an alternating voltage of suitable frequency. A moving-coil type vibration pick-up in

in contact with the plate then supplied an output voltage to the Y - plates of a cathode-ray oscilloscope, while an accurate oscillator connected to the X-plates provided a voltage of similar frequency. The frequency at which the plate was vibrating was obtained from the setting of the oscillator switches when a stationary ellipse was formed on the screen of the oscilloscope.

Resonance, and thus the required natural frequency, was found by altering the frequency of forced vibration until the output from the pickup was a maximum.

Modes of vibration were identified by investigating the nodal pattern at resonance, either by sprinkling sand on the surface of the plate or by moving the pick up across the plate.

Several experimental frequencies are shown in Table 2 where Warburton's notation has been used to identify the modes of vibration. The letters m and n refer respectively to the numbers of nodal lines parallel and perpendicular to the clamped edge of the plate (See Fig. 2). The calculated results given in the same table were obtained from Warburton's approximate method except for those modes of vibration with  $n = 1$ , where an approximation of the form

$$W(x,y) = A [\theta_m(x) + B \cdot \theta_{m+1}(x)] \cdot \phi_1(y)$$

has been used. The constant B was determined in such a manner as to minimise the frequency, and the following figures were obtained.

m	B
1	+ 0.2078
2	+ 0.2387
3	+ 0.1680

In the analysis of deflections and strains the same approximate mode shapes were used as in the calculation of natural frequencies. The value of A in the above two-term expression for W was chosen to make

$$\iint_a^b W^2 dx dy = ab$$

i.e.  $A^2 (1 + B^2) = 1$

or  $A = \frac{1}{\sqrt{1 + B^2}}$

This led to the following mode shapes, corresponding to the first six natural frequencies in numerical order.

$$W_1(x,y) = \theta_1(x) \cdot \phi_0(y)$$

$$W_2(x,y) = [0.9791 \theta_1(x) + 0.2035 \theta_2(x)] \phi_1(y)$$

$$W_3(x,y) = \theta_2(x) \cdot \phi_0(y)$$

$$W_4(x,y) = [0.9727 \theta_2(x) + 0.2322 \theta_3(x)] \phi_1(y)$$

$$W_5(x,y) = \theta_3(x) \cdot \phi_0(y)$$

$$W_6(x,y) = [0.9862 \theta_3(x) + 0.1657 \theta_4(x)] \phi_1(y)$$

#### 4.3. Transient Displacements

To record transient displacements of a point on the plate the apparatus shown in Fig. 6 was again used except for the vibration-generator and its associated oscillator.



The output voltage from the pickup was proportional to velocity so a "calibration unit" containing an integrating network was inserted between the pickup and the oscilloscope. This unit could also supply a voltage proportional to an amplitude of vibration (at the pickup) of  $10^{-3}$  of an inch.

One beam of the double-beam oscilloscope was used to display the transient signal while the decade oscillator supplied to the other beam a sinusoidal timing-signal of 1,000 c/s.

The oscilloscope screen was photographed on **35** m.m. film by a camera with a motor attachment which moved the film past the screen at an approximate speed of 25 inches per second.

The course of an experiment was as follows:

1. A photographic record was made of the standard amplitude of  $10^{-3}$  of an inch at 50 c/s.
2. A steel sphere was dropped from a suitable height on to the chosen point on the plate and a photographic record was made of part of the resultant free vibration at the position of the pickup. The sphere was allowed to rebound and to fall back to the plate surface.
3. The above procedure was repeated.

Part of the record, corresponding approximately to one cycle of the fundamental frequency of the plate, was then enlarged for comparison with calculated results.

When the sphere is allowed to fall back to the plate the second impact is clearly seen on the film. By using the timing signal on the film to measure the interval between first and second impacts a simple formula can be used to determine the coefficient of restitution. This formula depends on two assumptions which we may reasonably assume are satisfied.

1. The distance travelled by the sphere after the first impact is much greater than the movement of the plate at the impact point.
2. The velocity of the sphere on return to the plate surface is numerically equal to its velocity immediately after the first impact and is in the opposite direction.

Application of the laws of motion of a body moving freely under the action of gravity yields the formula,

$$e = \frac{g T_0}{2v}$$

$e$  = coefficient of restitution

$T_0$  = time interval between first and second impacts

$v$  = the speed of the sphere immediately before the first impact

$g$  = acceleration due to gravity.

It was found that the impact of the sphere produced a permanent deformation on the surface of the plate and under these conditions the coefficient of restitution was obtained as

$$e = 0.52$$



Data and calculated results are given below for the particular case of impact at the point with coordinates (6", 5½") and pickup at position (16", 7½")

Weight of sphere  $W = 0.01229$  lb

Radius of the sphere  $R = \frac{7}{32}$  "

Young's modulus for sphere and plate

$$E = 30 \times 10^6 \text{ lb/sq.in.}$$

Poisson's ratio for sphere and plate  $\nu = 0.3$

Length of the plate  $a = 16$  "

Breadth of the plate  $b = 7\frac{1}{2}$  "

Thickness of the plate  $h = 0.282$  "

Velocity of the sphere  $v = \sqrt{2g \times 15}$  "

$$= 107.7 \text{ in/sec.}$$

$$T = 3.23 \left[ \frac{\left(\frac{W}{g}\right)^2 (1-\nu^2)^2}{\nu R E^2} \right]^{\frac{1}{5}} = 27.3 \times 10^{-6} \text{ sec.}$$

The following tabulated values show the first five natural frequencies and the corresponding amplitudes of the associated terms in the series for displacement, equation (46).

Frequency	Amplitude
237 rad/sec.	+ 0.726 x 10 <sup>-3</sup> inches
1067	+ 0.284 x 10 <sup>-3</sup>
1485	- 0.370 x 10 <sup>-3</sup>
3411	- 0.199 x 10 <sup>-3</sup>
4162	+ 0.124 x 10 <sup>-3</sup>

Using the above five terms the displacement was evaluated at intervals of  $\frac{1}{2000}$  of a second for a total time of 25 milli-seconds. The resultant curve of displacement  $v$ , time is presented in Fig. 7 together

with the corresponding experimental result. Calculated and experimental curves are also presented in Fig. 8 for the displacement of the point at (16",0) due to impact at (6,5½).

#### 4.4. Transient Strains

Recordings of transient strains at a point on the surface of the plate were obtained with the apparatus shown in Fig. 9. The voltage across the strain gauge is

$$V_g = \frac{V \cdot R_g}{(R + R_g)}$$

where  $V$  = voltage of the battery = 24V

$R$  = resistance of the wirewound resistor

$R_g$  = resistance of the strain gauge.

Since the resistance of the gauge alters under strain we have a change in  $V_g$ ,

$$\begin{aligned} \delta V_g &= \frac{VR}{(R+R_g)^2} \cdot \delta R_g \\ &= \frac{R \cdot R_g}{(R+R_g)^2} \cdot V \cdot \frac{\delta R_g}{R_g} \\ &= \frac{R \cdot R_g}{(R+R_g)^2} \cdot V \cdot K \epsilon \end{aligned}$$

where  $K$  is the gauge factor, a constant for a particular gauge. The above equation shows that the change in voltage across the gauge is directly proportional to the strain. This voltage is then amplified and displayed on one beam of the oscilloscope while the other beam, as before, carries a timing signal.

Strains occurring at the position of gauge B (see Fig. 5) due to an impact at (6", 5 $\frac{1}{2}$ ") were calculated from equation (48) using the first five terms, the amplitudes of which were as shown below.

Frequency	Strain Amplitude
237 rad/sec	+ 1.329 x 10 <sup>-6</sup>
1067	- 0.694 x 10 <sup>-6</sup>
1485	+ 3.630 x 10 <sup>-6</sup>
3411	- 2.006 x 10 <sup>-6</sup>
4162	+ 2.897 x 10 <sup>-6</sup>

Calculated and experimental results for this problem and also for the strains at gauge A due to the same impact conditions are shown in Figs 10 and 11 respectively.

Due to the experimental method adopted only a qualitative comparison is possible of the experimental and theoretical strains.

m	A (Fig 7)	B (BARTON)	Ratio $\frac{A}{B}$
1	+ 0.8196	+ 0.8153	1.005
2	+ 1.4459	+ 1.4630	0.988
3	- 2.6154	- 2.4915	1.050
4	- 3.2254	- 3.6115	0.893
5	+ 2.4658	————	————

Figs. 7 and 8 show that the displacements calculated from five terms of the infinite series agree with the general trend of the experimental results during the first ten or twelve milli-seconds. After this period the differences between the curves become more noticeable and it is apparent that the development of the predicted history proceeds more quickly than that of the experimental result. Two of the more important causes of these differences are

- (a) calculated frequencies are higher than observed values  
and (b) normal mode shape approximations may be too simplified.

From equation (46) we see that displacement  $w$  is related to the mode shape  $W_m(x,y)$  by

$$w \propto W_m(x_0, y_0) \cdot W_m(x_1, y_1)$$

The figures given below compare the values of this product used in the calculations for Fig. 7. with improved values obtained from the nine-term series used by Barton.

$W_m(x_0, y_0) \cdot W_m(x_1, y_1)$			
$m$	A (FIG 7)	B (BARTON)	RATIO $\frac{A}{B}$
1	+ 0.8196	+ 0.8153	1.005
2	+ 1.4459	+ 1.4630	0.988
3	- 2.6154	- 2.4915	1.050
4	- 3.2254	- 3.6115	0.893
5	+ 2.4658	—	—

The coefficients required for the nine-term series were available only for the first four mode-shapes but these few results suggest that the error involved in using a one-term approximation is greater for the higher frequencies, and also that the amount of the error is not constant. It is the variation of error that causes distortion of the computed record since a constant % error would increase or decrease each term, and thus the total displacement, by the same factor.

Equation (46) relates displacement and frequency by

$$w \propto \frac{\cos \frac{\omega_m T}{\pi} \cdot \frac{\pi}{2}}{\left(\frac{\omega_m T}{\pi}\right) \left[1 - \left(\frac{\omega_m T}{\pi}\right)^2\right]} \cdot \sin \omega_m \left(t - \frac{T}{2}\right)$$

$$= G(\omega_m) \cdot \sin \omega_m \left(t - \frac{T}{2}\right), \text{ say.}$$

A constant % error in frequency would alter the time scale by the same factor but, in general, distortion would still result from error variations in the quantity  $G(\omega_m)$ .

Where the errors in estimating  $\omega_1, \omega_2, \omega_3, \dots$  etc, are different then some time after the start of the vibration the corresponding terms in the series for displacement may subtract instead of adding. This suggests why only the beginning of the calculated curve in Fig. 7 (Fig. 8) agrees reasonably well with the experimental result.

Values obtained for  $G(\omega_m)$  using (a) calculated frequencies, and (b) experimental frequencies are given below.

$G(\omega_m)$			
$m$	A (FIG7)	B (EXPERIMENTAL)	RATIO $\frac{A}{B}$
1	486	515	0.944
2	108	113	0.956
3	77.5	84	0.923
4	33.7	34.6	0.974
5	27.6	29.6	0.932

The results in the last two tables were used to re-calculate the amplitudes of the terms in the displacement series and Figs. 12 and 13 were drawn to correspond to Figs. 7 and 8

DISPLACEMENTS			
$m$	A (FIG7)	B (MODIFIED VALUES)	RATIO $\frac{A}{B}$
1	+ $0.726 \times 10^{-3}$ "	+ $0.766 \times 10^{-3}$ "	0.948
2	+ $0.284 \times 10^{-3}$ "	+ $0.302 \times 10^{-3}$ "	0.941
3	- $0.370 \times 10^{-3}$ "	- $0.382 \times 10^{-3}$ "	0.969
4	- $0.199 \times 10^{-3}$ "	- $0.228 \times 10^{-3}$ "	0.872
5	+ $0.124 \times 10^{-3}$ "	—————	—————

Even though only four terms were used for the new curves it is immediately obvious that the agreement with the experimental results is better. It is to be expected that the results in Figs. 12 and 13 would be improved even further by making use of more terms from the infinite series, but in Figs. 7 and 8 adding more terms based on approximate frequencies and mode shapes would/



would probably cause more distortion of the record.

If no damping were present it is possible that at some time the deflection would be obtained by adding the maximum values of each term in the series.

i.e. If

$$W = Y_1 \sin \omega_1 (t - \frac{T}{2}) + Y_2 \sin \omega_2 (t - \frac{T}{2}) + \dots$$

$$W_{max} = Y_1 + Y_2 + Y_3 + Y_4 + \dots$$

This is the formula derived by Greenspon as an upper limit for the maximum deflection. He assumes that in practice it is sufficient to consider only four terms and the calculations are based on the one-term approximate mode shape. The following figures compare the values obtained from this formula with the corresponding observed maximum, Fig. 7 or 12.

	$W_{max}$
ABOVE FORMULA : ONE-TERM MODE SHAPE	$1.491 \times 10^{-3} "$
" " : FIG 7 CALCULATIONS	$1.579 \times 10^{-3} "$
" " : FIG 12 "	$1.678 \times 10^{-3} "$
ACTUAL CALCULATED MAX. FOR FIG 7 (5 TERMS)	$1.42 \times 10^{-3} "$
" " " " FIG 12.	$1.40 \times 10^{-3} "$
OBSERVED MAX. FIG 7 OR 12.	$1.88 \times 10^{-3} "$

It can be seen that the experimental figure is larger than any of the estimates. Since the calculations are based on an approximate force and an experimental value of coefficient of restitution, comparison of the above results may not be helpful in criticising Greenspon's procedure. A method of initiating the transient vibration which could be "exactly" accounted for in the analysis would be necessary before reaching any relevant conclusions. One comment which can be made, however, is that in the above case the more exact calculations seem to give higher values of  $W_{max}$  than the simple one-term approximation, and each of these figures is greater than the actual calculated maximum deflection.

In a practical case the presence of damping will affect the amplitudes and  $W_{max}$  will occur during the first few cycles of the lower frequencies.

The integral equation developed for elastic, Hertzian impact of a sphere on a plate is similar to that obtained by Timoshenko for impact on a beam. In this latter case Timoshenko (1913) suggested that the problem of plastic impact could be treated in a similar manner provided that a static relationship between force and distance was known for the plastic condition.

In the plastic region the rate of straining is important and relaxation of stress and strain may not occur at the rate of removal of the load. In view of this the use of a static plastic relationship in the integral/

integral equation would be an approximation similar to the use of the Hertz expression for elastic impact.

Even with elastic impact it has been tacitly assumed that all the energy transmitted to the plate (or beam) results in flexural motion. That this is not necessarily so is shown by an investigation by Goodier and Ripperger (1959). A steel sphere of diameter  $2a$  was allowed to strike a steel slab of thickness  $h$  and records were taken of strains produced on the upper and lower surfaces of the slab. For  $\frac{h}{2a} > 16$  the motion was essentially confined to a surface wave on the upper face of the slab. i.e. The response was that of a semi-infinite solid rather than a thin plate. The motion was almost entirely flexural when  $\frac{h}{2a} < 3$ . In the intermediate range  $3 < \frac{h}{2a} < 16$  it would be necessary to consider both flexural and surface wave effects.

The present experiments were performed with  $\frac{h}{2a} \doteq 1$ .

Since strains are obtained from the series for displacement by differentiating with respect to one of the space variables,  $x$  or  $y$ , a process which increases the importance of the higher frequencies, it is to be expected that convergence of the resultant series will be slower than that of the series for displacement. i.e. More terms may be required to give a reasonable representation of the experimental result than is the case for displacements.

Observed/

Observed (qualitative) and predicted strains are presented in Figs. 10 and 11 for two cases. Both strain gauges were placed near the clamped edge of the plate (see Fig. 5) but one gauge was situated on the line of symmetry so that asymmetrical modes produced no effect. Fig. 11 shows the results for this gauge, the calculations being limited to consideration of only three frequencies. It should be noted that three of the first six natural frequencies correspond to asymmetrical mode shapes.

Many of the comments made about the displacement records in Figs. 7 and 8 can be repeated for Figs. 10 and 11. Approximate frequencies produce the same effect on strain and displacement but there is a difference in the effect of using approximate mode shapes. Strain  $\epsilon_x$  in the x-direction is related to mode shape  $W_m(x,y)$  by

$$\epsilon_x \propto W_m(x_0, y_0) \cdot \frac{\partial^2 W_m(x_2, y_2)}{\partial x^2}$$

Fig. 7 (displacement) and Fig. 10 (strain) were calculated from the same five mode shapes.

The four improved mode shapes obtained from the nine-term series of Barton were used to calculate Figs. 12 (displacement) and 14 (strain) but in the latter case, Fig. 14, it was found necessary to include/

include a fifth (approximate) shape. Values of the above product are compared in the following table

$W_m(x_0, y_0) \cdot \frac{\partial^2 W_m(x_2, y_2)}{\partial x^2}$			
m	A (FIG 10)	B (FIG 14)	RATIO $\frac{A}{B}$
1	+ 0.010637	+ 0.010459	1.017
2	- 0.025025	- 0.025920	0.965
3	+ 0.182080	+ 0.174687	1.042
4	- 0.231136	- 0.199647	1.158
5	+ 0.407704	+ 0.407704	1.000

The corresponding amplitudes of each term in the series for strain are:

STRAINS			
m	A (FIG 10)	B (FIG 14)	RATIO $\frac{A}{B}$
1	+ $1.3288 \times 10^{-6}$	+ $1.386 \times 10^{-6}$	0.959
2	- $0.69416 \times 10^{-6}$	- $0.754 \times 10^{-6}$	0.921
3	+ $3.6303 \times 10^{-6}$	+ $3.776 \times 10^{-6}$	0.961
4	- $2.0059 \times 10^{-6}$	- $1.777 \times 10^{-6}$	1.129
5	+ $2.8965 \times 10^{-6}$	+ $3.107 \times 10^{-6}$	0.932

The effect of the new figures for strain is to reduce the distortion in the later parts of the calculated history and to eliminate the reduction in time scale which arises from use of inaccurate frequencies. No great change is apparent in the calculated result for Fig. 15 when compared with Fig./

Fig. 11 except the change in time scale. This may be due to the use of only three terms and the fact that errors in approximate frequencies for symmetrical modes are more nearly constant than for asymmetrical modes, so that distortion would not be appreciable in that part of the record considered in Figs. 11 and 15.

Greenspon's method can be used to estimate the maximum strain and values obtained in this way are shown below for the case represented in Figs. 10 and 14. No experimental result is quoted since the method used to record strain did not provide quantitative results.

	$\epsilon_{x \max}$	
	FOUR TERMS	FIVE TERMS
GREENSPON'S FORMULA : ONE-TERM MODE SHAPE	$6.16 \times 10^{-6}$	$9.06 \times 10^{-6}$
" " : FIG 10 CALCULATIONS	$7.66 \times 10^{-6}$	$10.56 \times 10^{-6}$
" " : FIG 14 "	$7.69 \times 10^{-6}$	$10.8 \times 10^{-6}$
ACTUAL CALCULATED MAX. FOR FIG. 10	————	$9.73 \times 10^{-6}$
" " " " FIG. 14.	————	$8.38 \times 10^{-6}$

The similar table of results for displacement showed that the "upper limits" calculated by Greenspon's method were larger than the actual maxima as given by the calculated curves Fig. 7 and 12. The above table shows that this is not so for strains unless five terms are considered.

The analysis has neglected such factors as internal and external damping, rotatory inertia and shear/

shear deformation. The effect of damping in a practical case will be to eliminate the higher modes of vibration from the experimental records and, unless calculated results are required over several cycles of the lower frequencies, damping can usually be neglected. (The calculation being limited to consideration of the lower modes only). Shear deformation, and to a lesser extent rotatory inertia, will be important during the initial stages of the impact process when the disturbance is confined to a small region near the point of contact. Where information is required concerning shear forces (or the force between the sphere and plate) it would seem necessary to consider shear deformation. This would suggest that the integral equation of Timoshenko should be modified to include deflections due to both flexure and shear. Such a procedure would greatly complicate the analysis and it is doubtful whether, in general, the results obtained would justify the extra complexity.

Goland, Wickersham and Dengler (1955) investigated the problem of strain propagation in beams subjected to impulsive loading, including in their analysis the effects of rotatory inertia and shear deformation. A force gauge was designed in which a steel hemisphere rested on the surface of a Barium Titanate strain-gauge, which in turn was cemented to the surface of the beam. A steel sphere was allowed to fall on to this gauge and the resultant/

resultant variation of force was obtained from the changes of voltage generated by the Barium Titanate. This recorded force history was assumed to act as a series of impulses and as such was utilised in the mathematical analysis of the problem.

For the period during which the sphere was in contact with the beam strains calculated by this method showed good agreement with observed results except for a small-amplitude high-frequency component present in the measured strain histories but lacking in the analytical solution.

A similar method could be used to measure the force applied to a plate during impact instead of using the Zener-Feshbach procedure. It offers the possibility of dealing with cases where double-peaked force histories occur. (Sub-impacts).

While a variation of strain produces a similar variation of voltage across a Barium Titanate gauge attached to the strained surface, the opposite is also true. i.e. By supplying a suitable voltage pulse to the gauge it should be possible to apply to the surface of the plate a given transient strain. This suggestion has not been tested except for sustained harmonic motion but it would be an interesting method of inducing a transient vibration since pulses of almost any shape can be produced by electrical means.

Static deflection caused by a concentrated force

P/



P can be obtained from equation (39) by allowing  $\omega$  to tend to zero and considering the result at  $\omega t = \frac{\pi}{2}$

We have

$$w(x,y) = \frac{Pg}{\rho h ab} \sum \frac{W_m(x_0, y_0) \cdot W_m(x, y)}{\omega_m^2} \quad (49)$$

Taking  $(x, y) = (x_0, y_0) = (a, 0)$  and rewriting the equation non-dimensionally, we have for the deflection under the load at a free corner of a square cantilever plate,

$$\frac{D \cdot w(a, 0)}{P a^2} = \sum \frac{W_m^2(a, 0)}{\lambda_m^2 \pi^4} \quad (50)$$

Values of this quantity obtained by various methods are compared below

<b>LIVESLEY &amp; BIRCHALL : FINITE DIFFERENCES (a)</b>	<b>0.490</b>
<b>" " " " (b)</b>	<b>0.500</b>
<b>5 TERMS OF THE SUM IN EQUATION (50)</b>	<b>0.495</b>
<b>MACNEAL : ANALOGUE NETWORK</b>	<b>0.522</b>
<b>" : DIRECT MEASUREMENT</b>	<b>0.462</b>

The results of Livesley and Birchall (1956) were found using finite differences with a network of thirty-six points. (See Chapter 2, Section 2.2.6.) It is possible to use as boundary conditions on the clamped edge either (a) deflection and slope equal to zero, or (b) deflection zero and symmetry about the edge. Conditions (a) and (b) yield the corresponding/

corresponding figures in the above table.

One-term approximations were used for the mode shapes in equation (50) and the frequency parameters  $\lambda_m$  were evaluated by Warburton's method.

MacNeal's electrical analogue is essentially a sixteen-point finite-difference network and as such is less accurate than the procedure used by Livesley and Birchall.

Static deflections are important in a method suggested by Williams (1949) for obtaining displacements due to a transient load. The integral in equation (38) of Chapter 3 is evaluated by parts to give

$$w(x,y,t) = \sin \omega t \sum_{p,q,a,b} \frac{Pq}{\rho h a b} \frac{W_m(x_0, y_0) \cdot W_m(x, y)}{\omega_m^2} - \frac{Pq}{\rho h a b} \sum_{p,q,a,b} \frac{W_m(x_0, y_0) \cdot W_m(x, y)}{\omega_m^2} \left[ \frac{\sin \omega t - \left(\frac{\omega_m}{\omega}\right) \sin \omega_m t}{1 - \left(\frac{\omega_m}{\omega}\right)^2} \right] \quad (51)$$

The first sum is recognised as the static deflection due to the concentrated load P, and the remaining summation of terms is the additional effect produced by inertia forces.

The static deflection can be evaluated either by summing the series or by substituting a value from some other source. (e.g. Livesley and Birchall). According to Williams only a few of the inertial terms need be considered due to the rapid convergence of the series.

As a final comment it is perhaps relevant to note that while this dissertation is concerned only with a uniform rectangular plate, in practice it may be necessary/



APPENDIX 1

Application of Calculus of Variations to Minimise Equation (17)

With the notation  $W_{xx} = \frac{\partial^2 W}{\partial x^2}$ , etc,

we have

$$\omega^2 = \frac{\int_0^a \int_0^b \{ W_{xx}^2 + W_{yy}^2 + 2\nu W_{xx} W_{yy} + 2(1-\nu) W_{xy}^2 \} dx dy}{\frac{\rho h}{Dg} \int_0^a \int_0^b W^2 dx dy} \quad (17)$$

The right hand side of this equation is a functional of  $W, W_{xx}, W_{yy}$  and  $W_{xy}$ .  $x$  and  $y$  are considered as fixed quantities and only  $W$  and its derivatives are to be varied.

For  $\omega^2$  to be stationary the first variation must be zero.

$$\omega^2 = \frac{F_1}{F_2}$$

$$\therefore \delta(\omega^2) = \frac{F_2 \delta F_1 - F_1 \delta F_2}{F_2^2} = 0$$

$$\therefore \delta F_1 - \frac{F_1}{F_2} \delta F_2 = \delta F_1 - \omega^2 \delta F_2 = 0$$

$F_2$  does not contain derivatives of  $W$ , thus

$$\begin{aligned} \delta F_2 &= \frac{\partial F_2}{\partial W} \delta W \\ &= 2 \cdot \frac{\rho h}{gD} \int_0^a \int_0^b W \delta W dx dy \end{aligned}$$

$$\begin{aligned} \delta F_1 &= \frac{\partial F_1}{\partial W_{xx}} \delta W_{xx} + \frac{\partial F_1}{\partial W_{yy}} \delta W_{yy} + \frac{\partial F_1}{\partial W_{xy}} \delta W_{xy} \\ &= 2 \int_0^a \int_0^b \left\{ (W_{xx} + \nu W_{yy}) \delta W_{xx} + (W_{yy} + \nu W_{xx}) \delta W_{yy} + 2(1-\nu) W_{xy} \delta W_{xy} \right\} dx dy \end{aligned}$$

$$= 2 I_1 + 2 I_2 + 4(1-\nu) I_3, \text{ say.}$$

$$\therefore I_1 + I_2 + 2(1-\nu)I_3 - \frac{\rho h}{gD} \omega^2 \int_0^a \int_0^b W \cdot \delta W \cdot dx \cdot dy = 0 \quad (17a)$$

70.

$$I_1 = \int_0^a \int_0^b (W_{xx} + \nu W_{yy}) \frac{\partial^2}{\partial x^2} \delta W \cdot dx \cdot dy$$

Integrate by parts with respect to x, hence,

$$I_1 = \int_0^b [(W_{xx} + \nu W_{yy}) \delta W_x]_0^a \cdot dy - \int_0^b \int_0^a [W_{xxx} + \nu W_{xyy}] \delta W_x \cdot dx \cdot dy$$

Integrate the second integral by parts with respect to x,

$$I_1 = \int_0^b [(W_{xx} + \nu W_{yy}) \delta W_x]_0^a \cdot dy - \int_0^b [(W_{xxx} + \nu W_{xyy}) \delta W]_0^a \cdot dy - \int_0^a \int_0^b (W_{xxxx} + \nu W_{xxyy}) \delta W \cdot dx \cdot dy$$

Similarly, by interchanging x and y, and a and b,

we have

$$I_2 = \int_0^a [(W_{yy} + \nu W_{xx}) \delta W_y]_0^b \cdot dx - \int_0^a [(W_{yyy} + \nu W_{yxx}) \delta W]_0^b \cdot dx - \int_0^a \int_0^b (W_{yyyy} + \nu W_{xxyy}) \delta W \cdot dx \cdot dy$$

$$I_3 = \int_0^a \int_0^b W_{xy} \cdot \delta W_{xy} \cdot dx \cdot dy$$

Again, by parts with respect to x,

$$\begin{aligned} I_3 &= \int_0^a \int_0^b \{ [W_{xy} \delta W_y]_x - W_{xxy} \cdot \delta W_y \} \cdot dx \cdot dy \\ &= \int_0^a \int_0^b \{ [W_{xy} \delta W]_{xy} - [W_{xyy} \delta W]_x - [W_{xxy} \delta W]_y + [W_{xxyy} \delta W] \} \cdot dx \cdot dy \\ &= [ [W_{xy} \delta W]_0^a ]_0^b - \int_0^b [W_{xyy} \delta W]_0^a \cdot dy - \int_0^a [W_{xxy} \delta W]_0^b \cdot dx + \int_0^a \int_0^b W_{xxyy} \delta W \cdot dx \cdot dy \end{aligned}$$

Grouping terms together and substituting in (17a)

we find

$$\begin{aligned} \delta(\omega^2) &= \int_0^a \int_0^b [ \nabla^4 W - \frac{\rho h}{gD} \omega^2 W ] \delta W \cdot dx \cdot dy \\ &+ \int_0^a [ ( \frac{\partial^2 W}{\partial y^2} + \nu \frac{\partial^2 W}{\partial x^2} ) \delta W_y ]_0^b \cdot dx \\ &+ \int_0^b [ ( \frac{\partial^2 W}{\partial x^2} + \nu \frac{\partial^2 W}{\partial y^2} ) \delta W_x ]_0^a \cdot dy \end{aligned}$$

$$\begin{aligned}
& - \int_0^a \left[ \left( \frac{\partial^3 W}{\partial y^3} + (2-\nu) \frac{\partial^3 W}{\partial y \partial x^2} \right) \delta W \right]_0^b dx \\
& - \int_0^b \left[ \left( \frac{\partial^3 W}{\partial x^3} + (2-\nu) \frac{\partial^3 W}{\partial x \partial y^2} \right) \delta W \right]_0^a dy \\
& + 2(1-\nu) \left[ \left[ \frac{\partial^2 W}{\partial x \partial y} \cdot \delta W \right]_0^a \right]_0^b \\
& = 0
\end{aligned}$$

For this to be true each of the bracketed terms must vanish.

Therefore

$$\nabla^4 W - \frac{\rho R}{gD} \cdot \omega^2 W = 0 \quad \text{--- (11)}$$

and, on edges  $y = 0$  &  $y = b$

$$\frac{\partial^2 W}{\partial y^2} + \nu \frac{\partial^2 W}{\partial x^2} = 0 \quad \text{or} \quad \delta W_y = 0$$

$$\frac{\partial^3 W}{\partial y^3} + (2-\nu) \frac{\partial^3 W}{\partial y \partial x^2} = 0 \quad \text{or} \quad \delta W = 0$$

on edges  $x = 0$  &  $x = a$

$$\frac{\partial^2 W}{\partial x^2} + \nu \frac{\partial^2 W}{\partial y^2} = 0 \quad \text{or} \quad \delta W_x = 0$$

$$\frac{\partial^3 W}{\partial x^3} + (2-\nu) \frac{\partial^3 W}{\partial x \partial y^2} = 0 \quad \text{or} \quad \delta W = 0$$

and at the corners  $(x, y) = (0, 0); (a, 0); (0, b); (a, b)$

$$\frac{\partial^2 W}{\partial x \partial y} = 0 \quad \text{or} \quad \delta W = 0$$

(17b)

Thus we see that the function  $W$  which minimises equation (17) is a solution of equation (11), subject to the relevant boundary conditions in (17b).

For clamped edges,  $\delta W = \delta W_x$  (or  $\delta W_y$ ) = 0

For supported edges  $\delta W = 0$ ,  $\delta W_x \neq 0$

For free edges  $\delta W \neq 0$ ,  $\delta W_x \neq 0$

At a free corner

$\delta W \neq 0$ .

APPENDIX 2

References

In the cases where the variation is zero, e.g. where zero slope or deflection is prescribed at the boundary, the boundary conditions of equation (17b) are satisfied. Where the variation is not zero then the more complicated expressions in (17b) are the required boundary conditions which the function W must satisfy.

The above problem refers to a function W which makes  $\omega^2$  stationary. Further investigation shows that  $\omega^2$  is a minimum (Courant and Hilbert, 1953).

Briner, H. A.; McGowan, G. D. and Warren, C. E. (1943) J. App. Mechs., Trans. A.S.M.E., vol 57, pp. A135-143; A New Device for the Solution of Transient Vibration Problems by the Method of Electrical-Mechanical analogy.

Courant, R. and Hilbert, D. (1953) Methods of Mathematical Physics, Vol. 1, 1st English Edition, Interscience Publishers, New York and London.

Erington, A. G. (1953) J. App. Mechs., Trans. A.S.M.E. Vol. 75, pp. 461-466; Transverse Impact on Beams and Plates.

Goland, M.; Wickschman, P. D. and Degler, M.A. (1955) J. App. Mechs., Trans. A.S.M.E. Vol. 77, pp. 1-7; Propagation of Elastic Impact in Beams in Bending.

Goodier, J. N. and Ripperger, H. A. (1959) J. App. Mechs., Trans. A.S.M.E. Vol. 81, (Brief Note) pp. 146-147; Response of a Slab to Impact. Trans.

APPENDIX 2References

- Abramson, H. N. (1958) The Dynamics of Airplanes, The Ronald Press Company, New York.
- Arnold, R. N. (1937) Proc. I. Mech. E., vol. 137, pp.217-281, Impact Stresses in a Freely-supported Beam.
- Barton, M. V. (1951) J. App. Mechs., Trans. A.S.M.E. Vol. 73, pp.129-134; Vibration of Rectangular and Skew Cantilever Plates.
- Bishop, R. E. D. and Johnson, D.C. (1956) Vibration Analysis Tables, Cambridge University Press.
- Criner, H. E.; McCann, G. D. and Warren, C. E. (1945) J. App. Mechs., Trans. A.S.M.E., vol 67, pp.A135-141; A New Device for the Solution of Transient Vibration Problems by the Method of Electrical-Mechanical Analogy.
- Courant, R. and Hilbert, D. (1953) Methods of Mathematical Physics, Vol. 1, 1st English Edition, Interscience Publishers, New York and London.
- Eringen, A. C. (1953) J. App. Mechs., Trans. A.S.M.E. Vol. 75, pp.461-468; Transverse Impact on Beams and Plates.
- Goland, M.; Wickersham, P. D. and Dengler, M.A. (1955) J. App. Mechs., Trans. A.S.M.E. Vol. 77, pp.1-7; Propagation of Elastic Impact in Beams in Bending.
- Goodier, J. N. and Ripperger, E. A. (1959) J. App. Mechs., Trans. A.S.M.E. Vol.81, (Brief Note) pp.146-147; Response of a Slab to Impact. Transition from Surface Wave to Flexural Behaviour



- Greenspon, J. E. (1955) The David W. Taylor Model Basin, Report 774; Stresses and Deflections in Flat, Rectangular Plates under Dynamic Lateral Loads Based on Linear Theory.
- Hertz, H. (1881) J. für Math. (Crelle), Vol. 92, p.156; Über die Berührung fester elastischer Körper.
- Jones, R. P. N. (1954) J. App. Mechs., Trans. A.S.M.E., Vol. 76, pp.75-80; The Wave Method for Solving Flexural Vibration Problems.
- Lee, E. H. (1940) J. App. Mechs., Trans. A.S.M.E., Vol. 62, pp.A.129-138. Impact of a Mass Striking a Beam.
- Livesley, R. K. and Birchall, P.C. (1956).  
R.A.E. Technical Note No: M.S.26; Analysis of a Loaded Cantilever Plate by Finite Difference Methods.
- MacNeal, R. H. (1951) J. App. Mechs. Trans. A.S.M.E., Vol. 73, pp.59-67; The Solution of Elastic Plate Problems by Electrical Analogies.
- McCann, G. D. and MacNeal, R. H. (1950) J. App. Mechs., Trans. A.S.M.E., Vol.72, pp.13-26; Beam-vibration Analysis with the Electric-Analog Computer.
- Martin, A. I. (1956) Quart. J. Mech. and App. Math., Vol. IX, pp.94-102; On the Vibration of a Cantilever Plate.
- Mason, H. L. (1936) J. App. Mechs., Trans. A.S.M.E., Vol. 58, pp.A55-61; Impact on Beams.

Nothmann, G. A. (1948) J. App. Mechs., Trans. A.S.M.E.  
Vol. 70, pp.327-334; Vibration of a Cantilever  
Beam with Prescribed End Motion.

Rayleigh, Lord (1894) Theory of Sound, Vol. 1,  
2nd Edition, reprinted 1945 by Dover Publications,  
New York.

Rayleigh, Lord (1906) Phil. Mag., Series 6, Vol 11,  
p.283; On the Production of Vibrations by Forces  
of Relatively Long Duration with Application to  
the Theory of Collisions.

Ritz, W. (1909) Annalen der Physik, 4th Series, Vol.28  
p.737; Theorie der Transversalschwingungen  
einer quadratischen Platte mit freien Rändern.

See also

Kantorovich, L.V. and Krylov, V.I. (1958)  
Approximate Methods of Higher Analysis, pp.301-303;  
P. Noordhoff Limited, Groningen.

Stowell, E. Z.; Schwartz, E.B. and Houbolt, J.C. (1945)  
N.A.C.A. Report No.828; Bending and Shear Stresses  
Developed by the Instantaneous Arrest of the Root  
of a moving Cantilever Beam.

Timoshenko, S. (1913) Zeit. Math. u. Physik., Vol.62,  
pp.198-209. Reprinted in Collected Works (1953)  
pp.225-236, McGraw-Hill Book Company. Zur  
Frage nach der Wirkung eines Stoszes auf einen  
Balken.

Timoshenko, S. (1940) Theory of Plates and Shells,  
1st Edition, McGraw-Hill Book Company.

- Timoshenko, S. and Goodier, J.N. (1950) Theory of Elasticity, 2nd Edition, McGraw-Hill Book Company.
- U.S. Dept. of Commerce (1955) Tables of Sines and Cosines for Radian Arguments; National Bureau of Standards Applied Maths, Series 43.
- Warburton, G. B. (1954) Proc. I. Mech. E., Vol.168, pp.371-384; The Vibration of Rectangular Plates.
- Williams, D. (1949) The Aeronautical Quarterly, Vol.1 pp.123-136; Displacements of a Linear Elastic System under a given Transient Load.
- Williams, D. (1957) R.A.E. Report Structures 225, A New Method of obtaining lower limits for the Solutions of 'Eigenvalue' Problems for Beams and Plates.
- Young, D. (1950) J. App. Mechs., Trans. A.S.M.E., Vol.72, pp.448-453; Vibration of Rectangular Plates by the Ritz Method.
- Zener, C. and Feshbach, H. (1939) J. App. Mechs., Trans. A.S.M.E., Vol.61, pp.A67-70; A Method of Calculating energy losses during impact.

A area of beam cross-section  
 $A_{nn}$  dimensional coefficient in series for  $w(x,y,t)$ , equation (20)  
 B dimensional coefficient in two-term mode shape  
 D plate stiffness =  $\frac{EA^3}{12(1-\nu^2)}$   
 E Young's modulus of elasticity  
 $F(x,y,t)$  load per unit area acting on the plate

## Appendix 3

## Notation

$a, b$	dimensions of the plate in the x-and y- directions
$c$	$= \sqrt{\frac{EI_0}{AP}}$ = constant for a given beam
$e$	coefficient of restitution = $-\frac{2}{3}$
$g$	acceleration due to gravity
$h$	thickness of the plate
$k$	coefficient in Hertz expression, equation (26)
$l$	length of a beam; grid spacing in finite- difference method.
$i, k, m, n, \}$ $p, q, r, s$	positive integers
$q_r(t)$	generalised coordinate, equation (31)
$t$	time
$v, v_i$	velocities of the sphere
$w(x, t)$	deflection of a beam
$w(x, y, t)$	deflection of a plate
$x, y$	coordinates in rectangular, cartesian system
$(x_0, y_0)$	coordinates at the point of impact
$(x_1, y_1)$	coordinates at the position of the pickup.
$(x_2, y_2)$	coordinates at the position of the strain- gauge.
$A$	area of beam cross-section
$A_{mn}$	dimensionless coefficient in series for $W(x, y)$ , equation (20)
$B$	dimensionless coefficient in two-term mode shape
$D$	plate stiffness = $\frac{ER^3}{12(1-\nu^2)}$
$E$	Young's modulus of elasticity
$F(x, y, t)$	load per unit area acting on the plate

$\left. \begin{matrix} G_x, G_y, H_x, \\ H_y, J_x, J_y \end{matrix} \right\}$  factors in the equation for  $\lambda$ , equation (19)  
and Table 1.

$I$	second moment of area of beam cross-section
$K_r$	$= \sqrt{\frac{\omega_r}{c}}$ for a beam
$P, P(t)$	force between bodies in contact
$P(t)$	concentrated force acting on the plate
$\bar{P}(t)$	"normalised" force
$P_{HM}$	maximum value of Hertz force
$R$	radius of the sphere
$T$	kinetic energy of vibrating plate or beam
$T$	duration of application of $P(t)$
$T_H$	Hertz time of contact, equation (47)
$U$	strain energy of vibrating plate or beam
$W$	weight of the sphere
$W_r$	deflection at point $r$ in finite-difference network, Fig. 3.
$W_r(x)$	shape of $r$ th mode of vibration of beam, equation (3)
$W_r(x,y)$	shape of $r$ th mode of vibration of the plate
$\alpha$	change in distance between centres of two elastic bodies in contact, equation (26)
$E_x$	strain in the $x$ -direction at the surface of the plate
$\vartheta_m(x)$	$W_m(x)$ for a cantilever (clamped-free) beam, equation (13)
$\lambda$	frequency parameter, equation (18)
$\nu$	Poisson's ratio
$\rho$	weight density of the material of beam, plate and sphere.

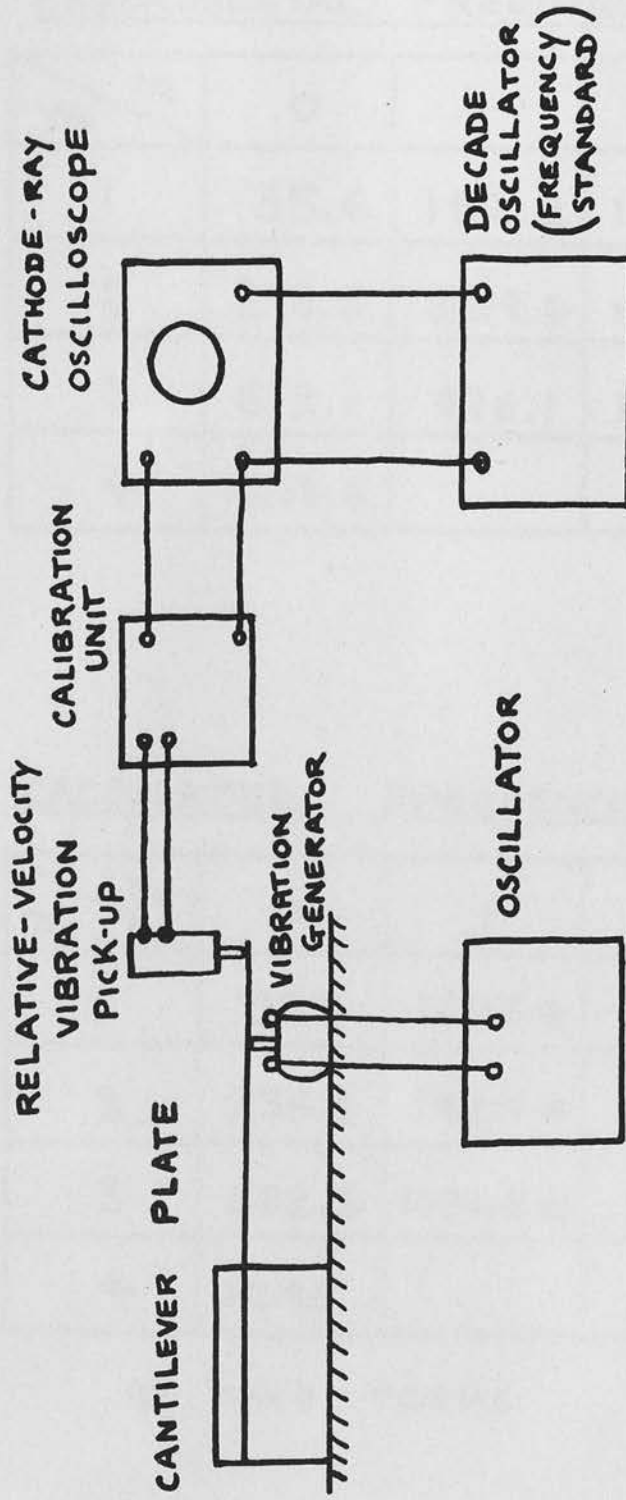
$\sigma_r$  parameter in equation (5) for  $W_r(x)$   
 $\phi_n(y)$   $W_n(y)$  for free-free beam, equation (14)  
 $\omega_r$  rth natural frequency radians per sec

$$\nabla^4 w = \frac{\partial^4 w}{\partial x^4} + 2 \frac{\partial^4 w}{\partial x^2 \partial y^2} + \frac{\partial^4 w}{\partial y^4}$$

PLATE DIMENSIONS AND CLIPPING ARRANGEMENT

FIG. 5





DETERMINATION OF NATURAL FREQUENCIES  
RECORDING OF TRANSIENT DISPLACEMENTS

FIG. 6



EXPERIMENTAL FREQUENCIES (c/s)

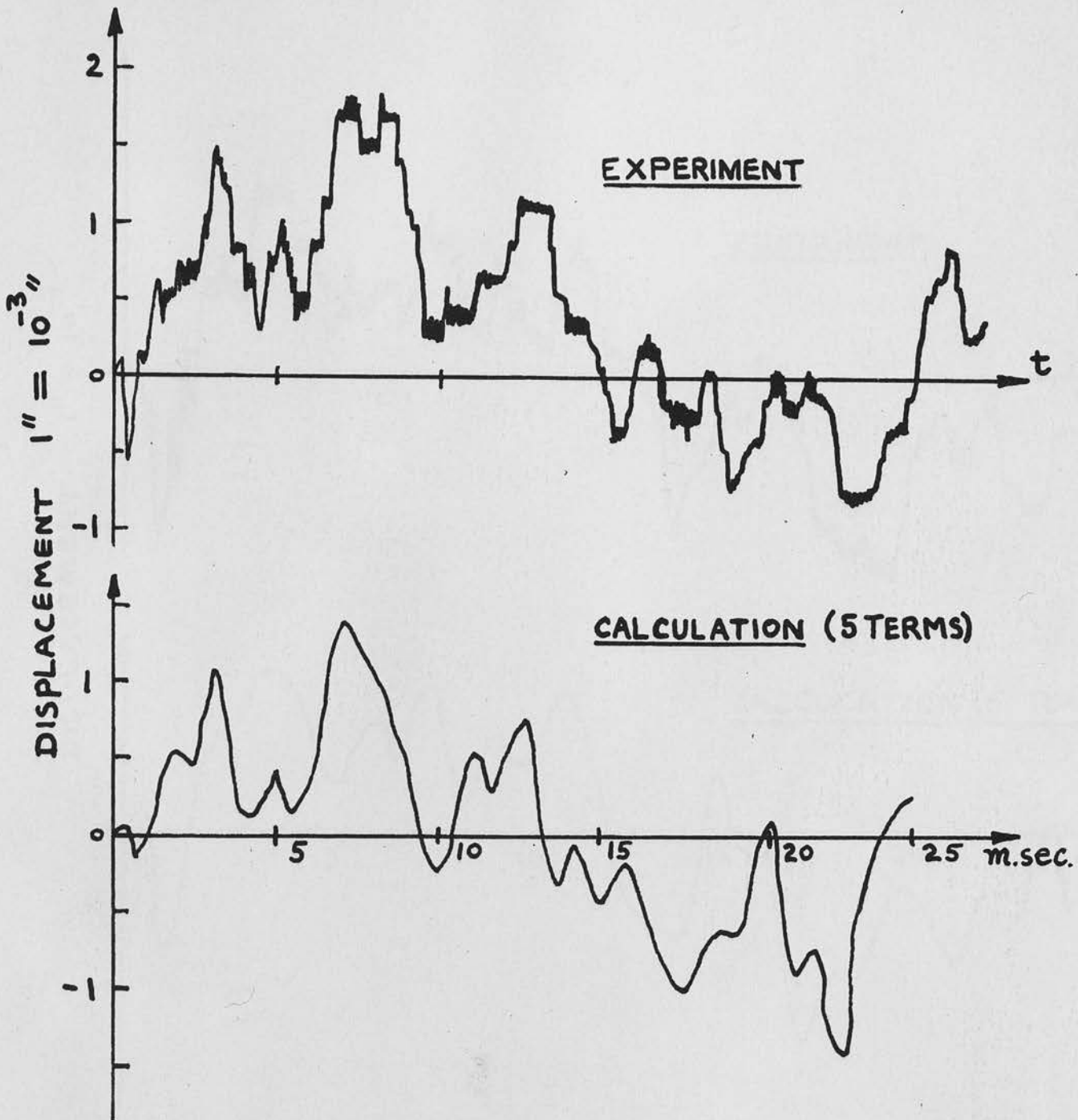
$m \backslash n$	0	1	2
1	35.6	162.2	1115.4
2	218.5	529.4	1451.3
3	618.1	996.1	1995.5
4	1215.8		

CALCULATED FREQUENCIES (c/s)

$m \backslash n$	0	1	2
1	37.7	169.8 *	1166
2	236.3	542.9 *	1563
3	662.3	1030.5 *	2149
4	1298		

\* TWO TERMS

TABLE 2.



DISPLACEMENT AT (16", 7½")

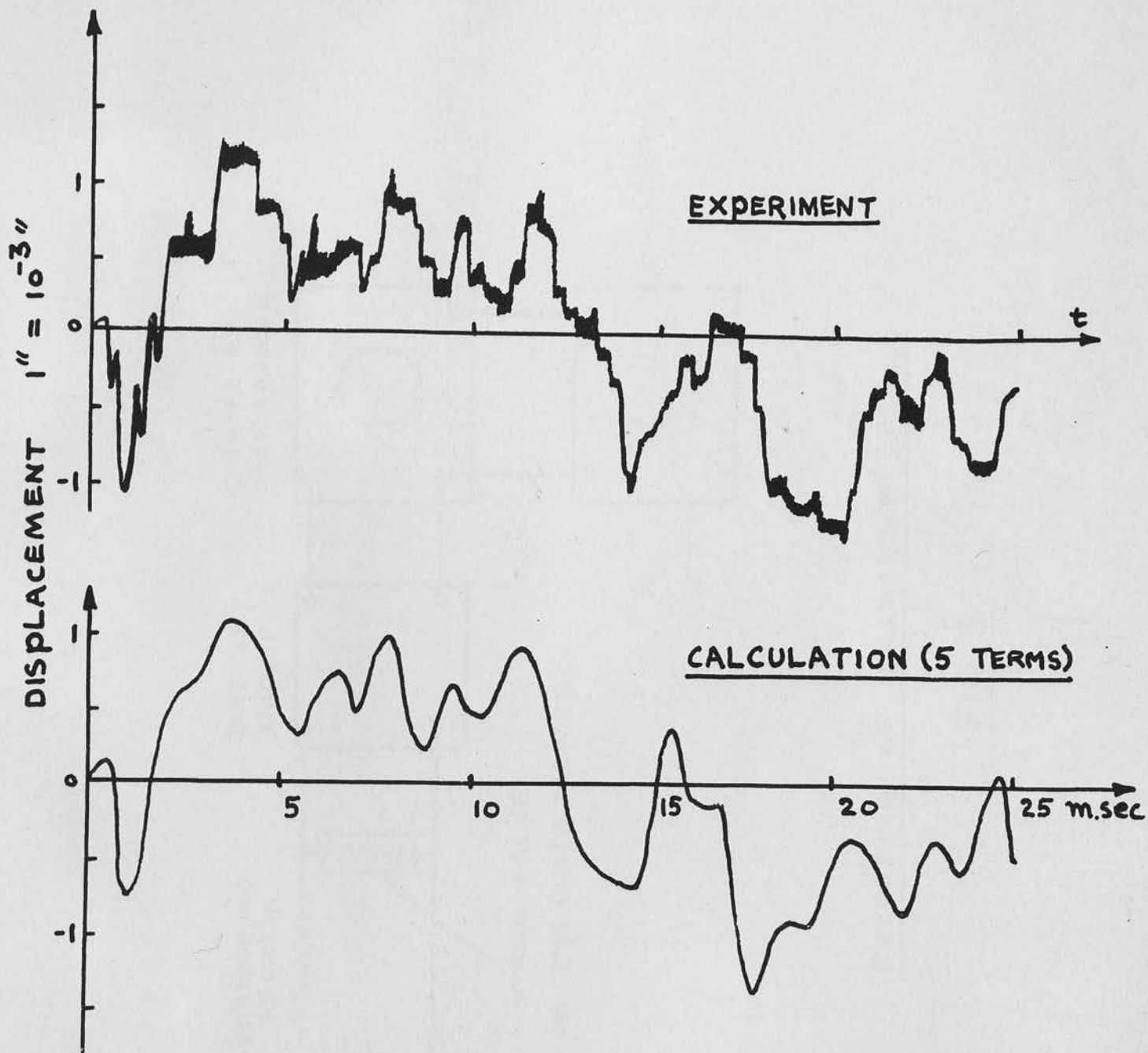
IMPACT AT (6", 5½")

$$v = 107.7 \text{ "/sec.}$$

$$W = 0.01229 \text{ lb}$$

$$R = \frac{7}{32} \text{ "}$$

FIG. 7



DISPLACEMENT AT (16", 0")

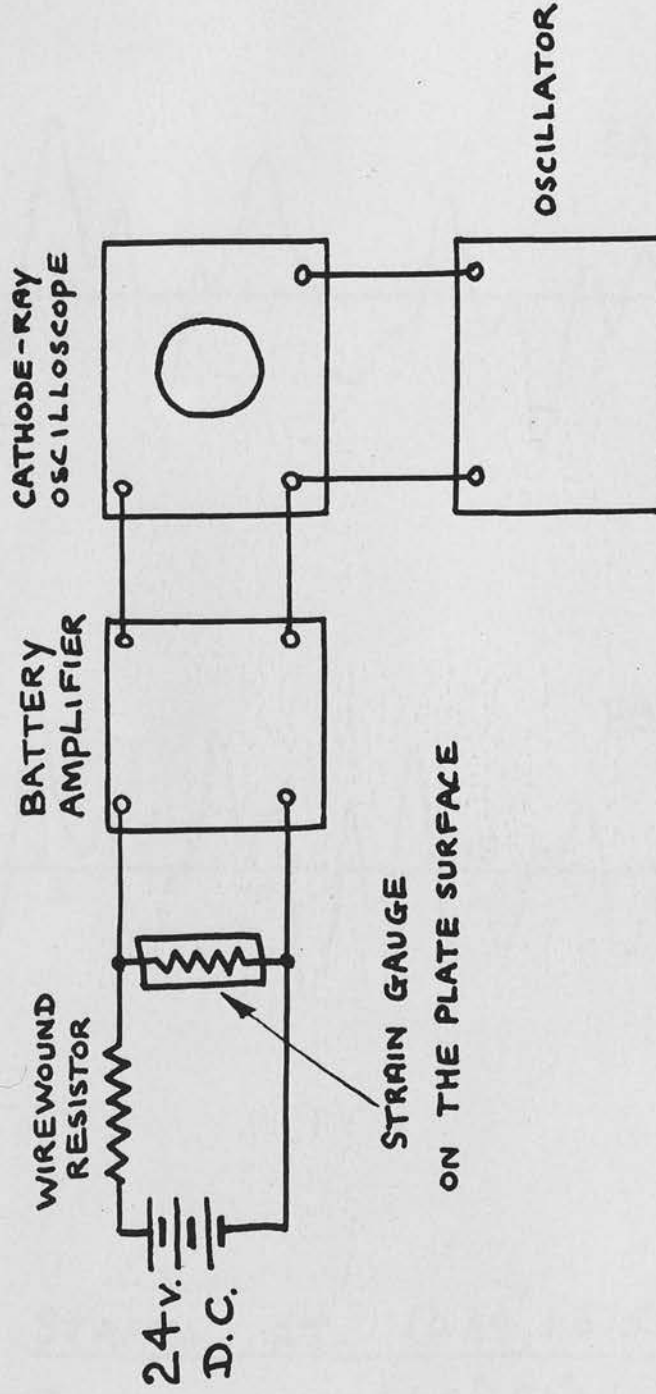
IMPACT AT (6", 5½")

$$v = 107.7 \text{"/sec.}$$

$$W = 0.01229 \text{ lb}$$

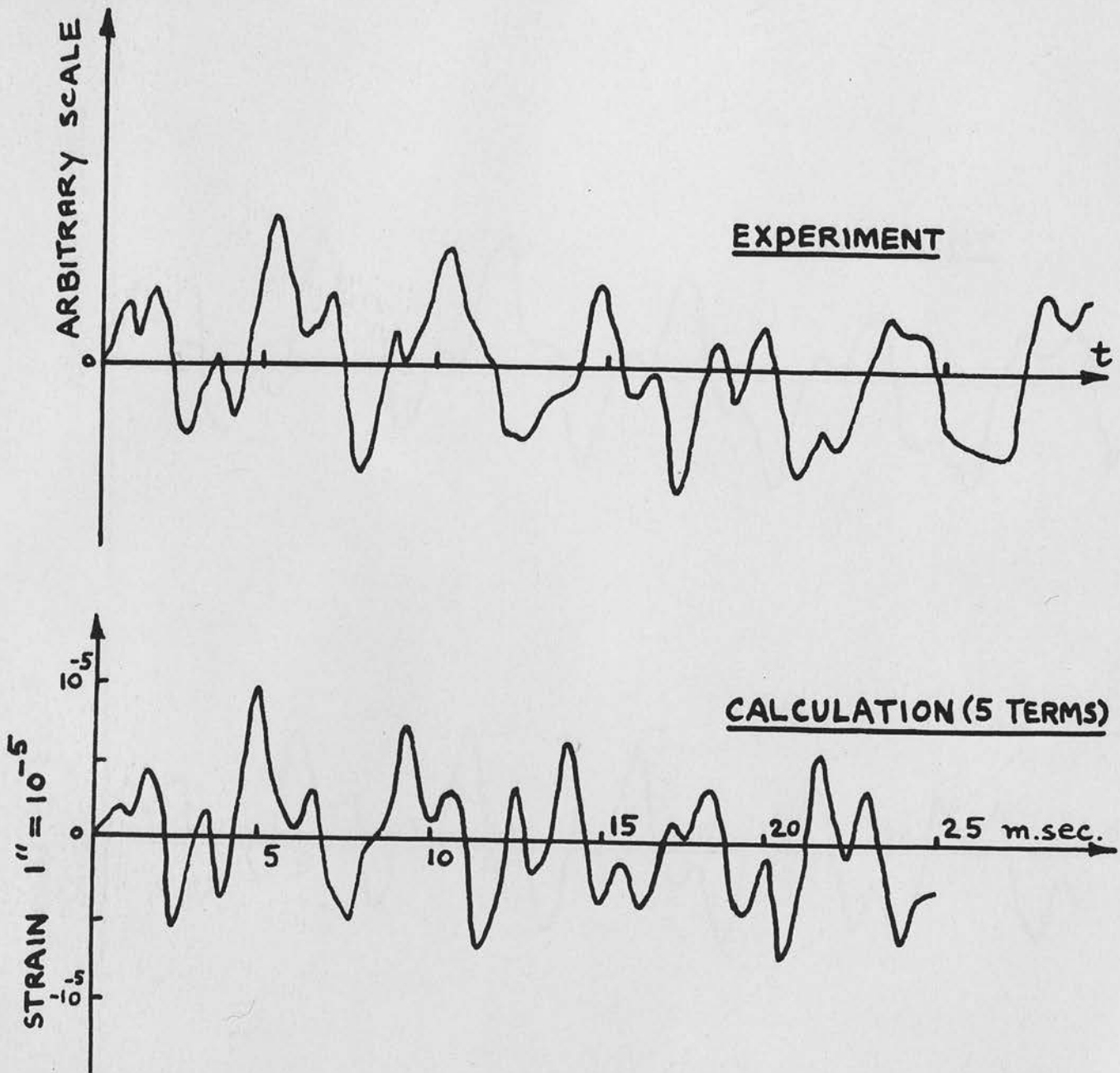
$$R = \frac{7}{32} \text{''}$$

FIG. 8



RECORDING OF TRANSIENT STRAINS

FIG. 9



STRAIN AT (0.64", 1.875")

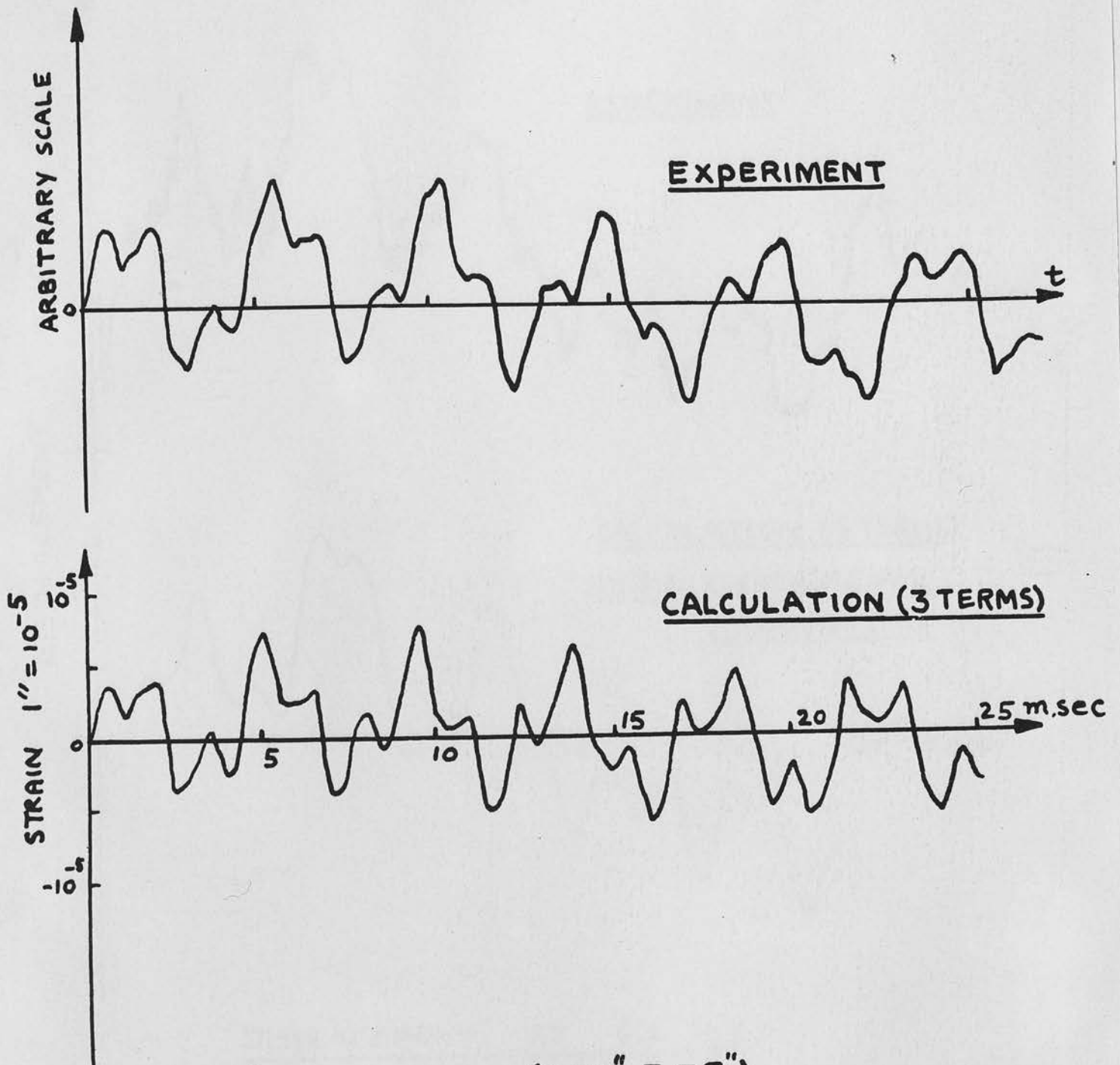
IMPACT AT (6", 5½")

$$v = 107.7 \text{ "/sec.}$$

$$W = 0.01229 \text{ lb}$$

$$R = \frac{7}{32} \text{ "}$$

FIG. 10



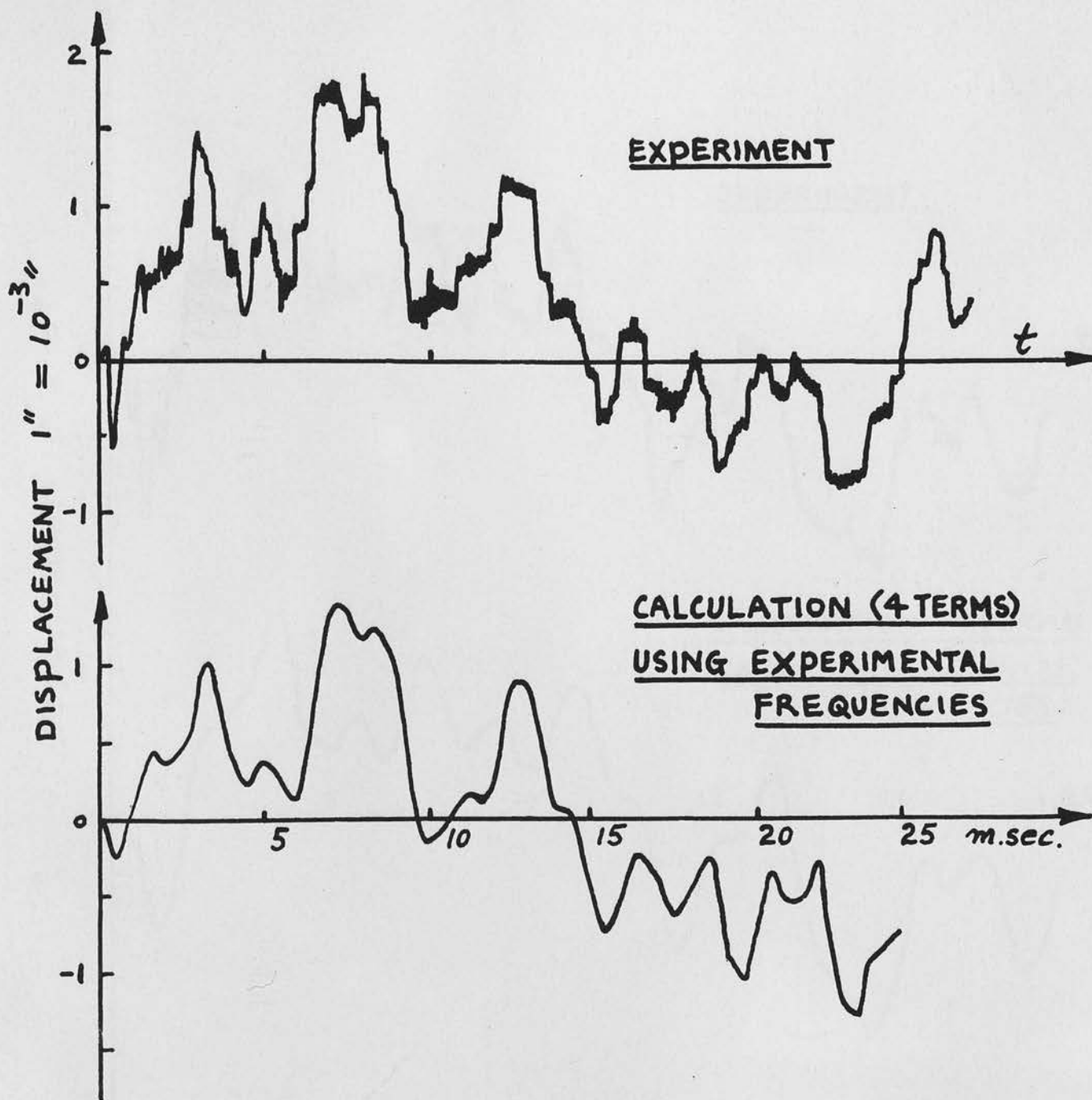
STRAIN AT (0.64", 3.75")  
IMPACT AT (6", 5½")

$$V = 107.7 \text{ "/sec.}$$

$$W = 0.01229 \text{ lb}$$

$$R = \frac{7}{32} \text{ "}$$

FIG. 11



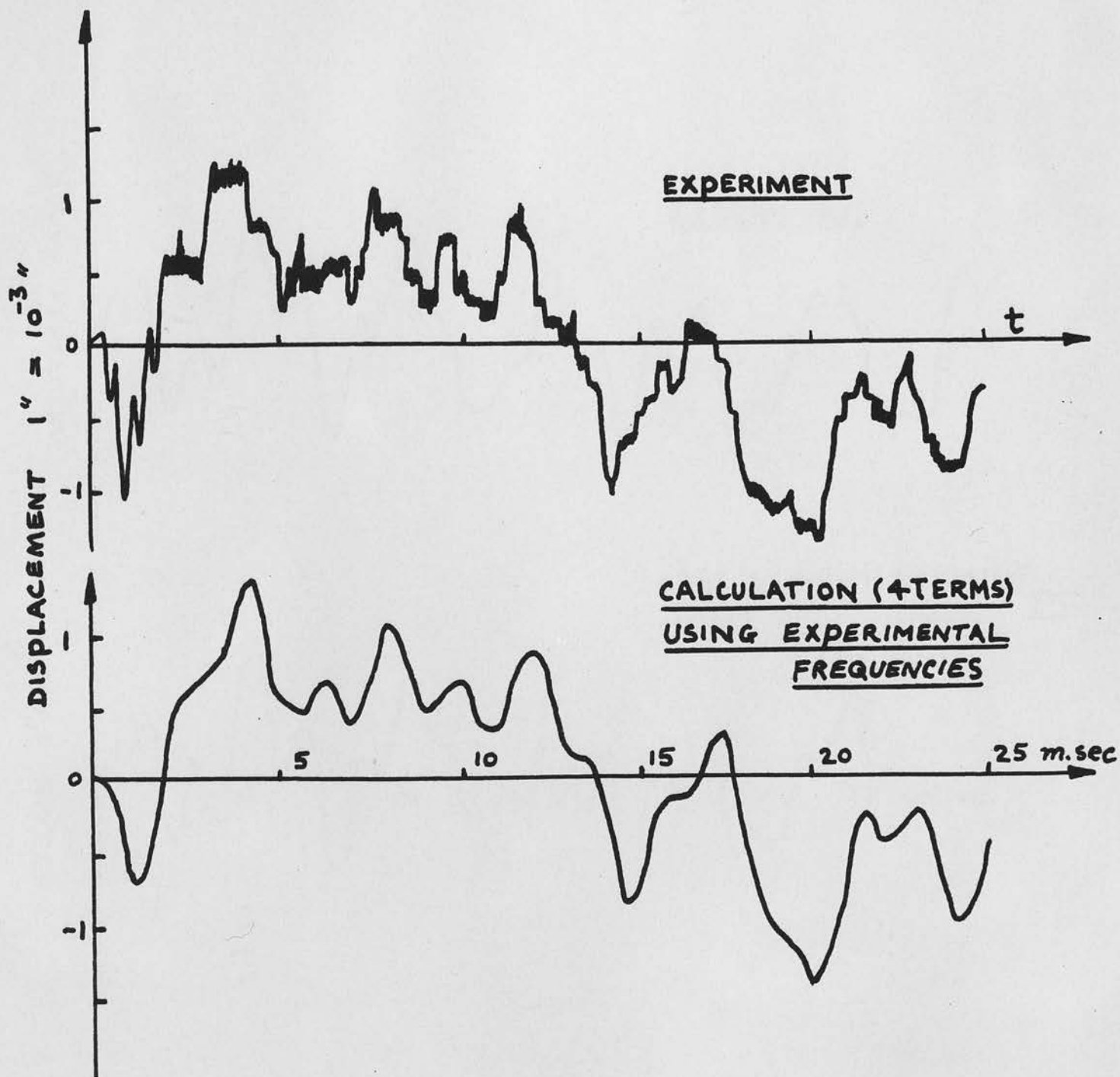
DISPLACEMENT AT (16", 7½")  
IMPACT AT (6", 5½")

$$V = 107.7 \text{ "/sec.}$$

$$W = 0.01229 \text{ lb}$$

$$R = \frac{7}{32} \text{ "}$$

FIG. 12  
(COMPARE FIG. 7)



DISPLACEMENT AT (16", 0")  
IMPACT AT (6", 5½")

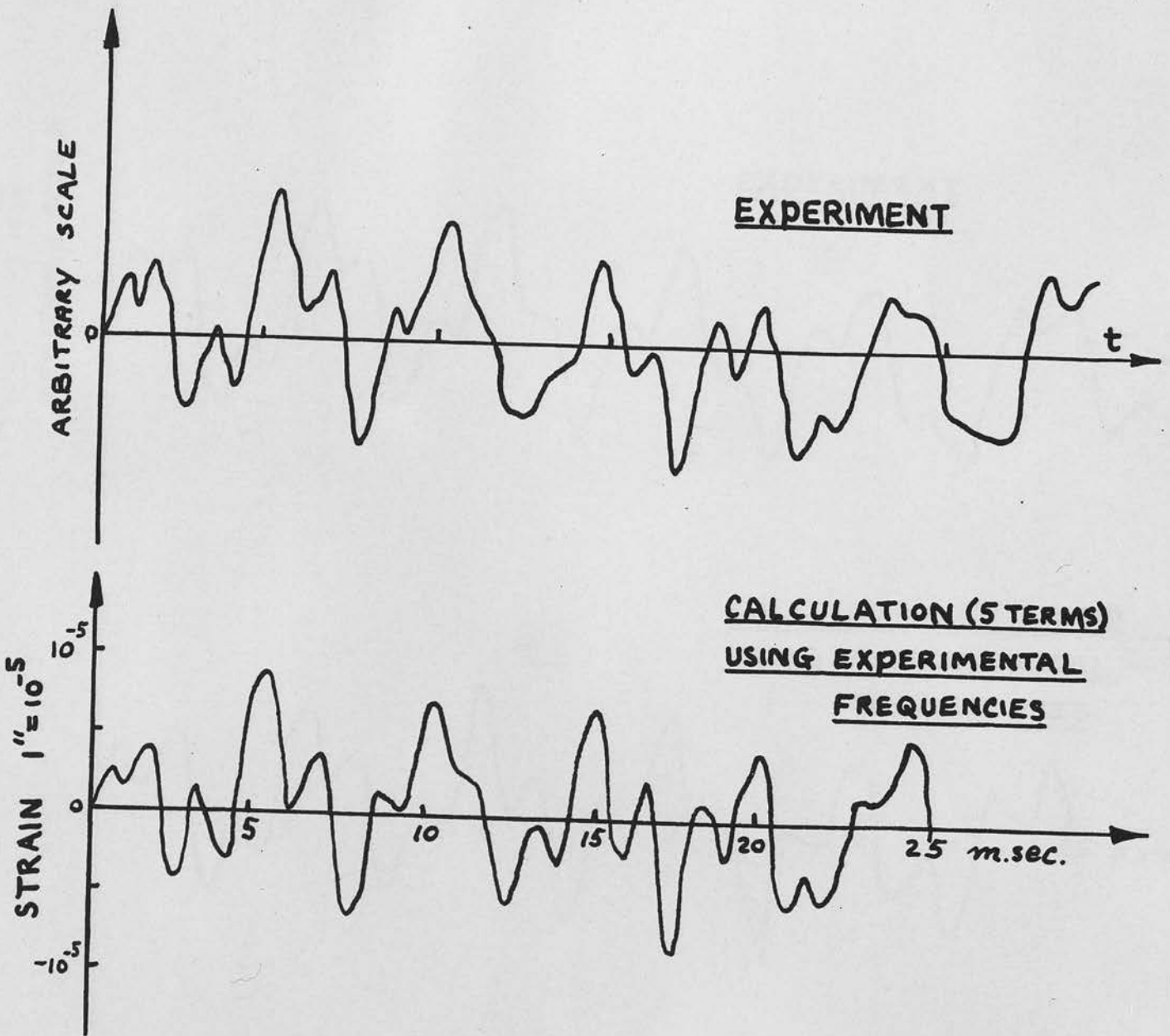
$$V = 107.7 \text{"/sec}$$

$$W = 0.01229 \text{ lb}$$

$$R = \frac{7}{32} \text{ "}$$

FIG. 13  
(COMPARE FIG. 8)

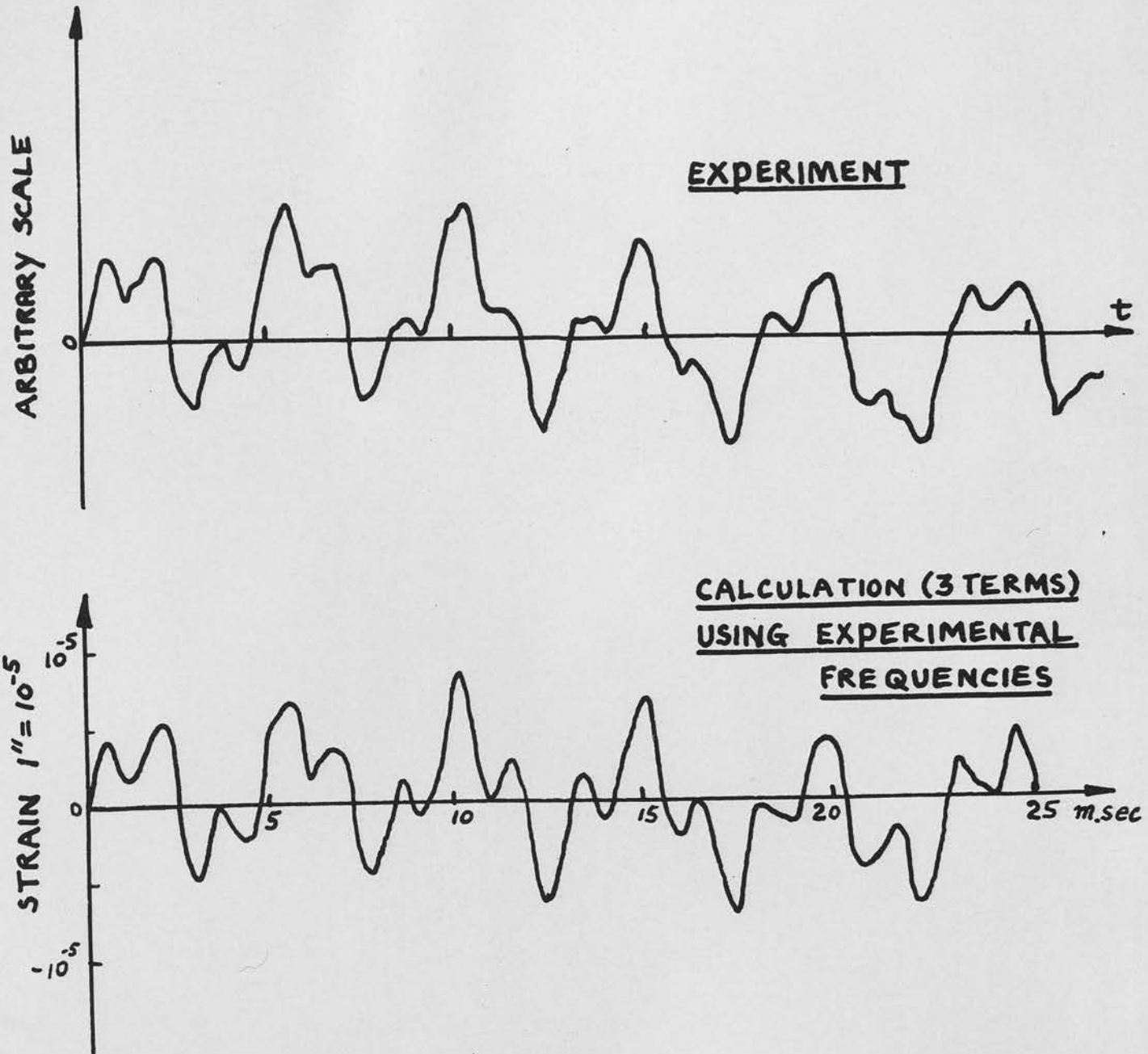




STRAIN AT (0.64", 1.875")  
IMPACT AT (6", 5 1/2")

$V = 107.7$ "/sec.  
 $W = 0.01229$  lb  
 $R = \frac{7}{32}$ "

FIG. 14  
(COMPARE FIG 10)



STRAIN AT (0.64", 3.75")  
IMPACT AT (6", 5½")

$$V = 107.7 \text{"/sec.}$$

$$W = 0.01229 \text{ lb}$$

$$R = \frac{7 \text{''}}{32}$$

FIG. 15  
(COMPARE FIG 11)